Frequent mutated B2M, EZH2, IRF8, and TNFRSF14 in primary bone diffuse large B-cell lymphoma reflect a GCB phenotype

de Groen, Ruben Al; van Eijk, Ronald; Boehringer, Stefan; van Wezel, Tom; Raghoo, Richard; Ruano, Dina; Jansen, Patty M; Briaire-de Bruijn, Inge; de Groot, Fleur A; Kleiverda, Karin

Published in:
Blood Advances

DOI:
10.1182/bloodadvances.2021005215

blood advances

American Society of Hematology
2021 L Street NW, Suite 900,
Washington, DC 20036
Phone: 202-776-0544 | Fax 202-776-0545
bloodadvances@hematology.org

Frequent mutated B2M, EZH2, IRF8, and TNFRSF14 in primary bone diffuse large B-cell lymphoma reflect a GCB phenotype

Tracking no: ADV-2021-005215-T

Ruben de Groen (Leiden UMC, Netherlands) Ronald van Eijk (LUMC, Netherlands) Stefan Boehringer (Leiden University Medical Center, Netherlands) Tom van Wezel (Leiden University Medical Center, Netherlands) Richard Raghoo (Leiden University Medical Center, Netherlands) Dina Ruano (Leiden University Medical Center, Netherlands) Patty Jansen (Leiden University Medical Center, Netherlands) Inge Briaire-de Bruijn (Leiden University Medical Center, Netherlands) Fleur de Groot (Leiden University Medical Center, Netherlands) Karin Kleiverda (Leiden University Medical Center, Netherlands) Liane te Boome (Haaglanden Medical Centre, Netherlands) Valeska Terpstra (Haaglanden Medical Center, Netherlands) Henriette Levenga (Groene Hart Hospital, Netherlands) Alina Nicolae-Cristea (Groene Hart Hospital, Netherlands) Eduardus Posthuma (Reiner de graaf Hospital, Netherlands) Isabelle Focke-Snieders (Reinier de Graaf Group, Netherlands) Lizan Hardi (Alrijne Hospital, Netherlands) Wietske den Hartog (Alrijne Hospital, Netherlands) Lara Bohmer (Haga hospital, Netherlands) Pancras Hogendoorn (Leiden University Medical Center, Netherlands) Anke van den Berg (University Medical Center Groningen, University of Groningen, Netherlands) Arjan Diepstra (University Medical Center Groningen, Netherlands) Marcel Nijland (University Medical Center Groningen, Netherlands) Pieternella Lugtenburg (Erasmus MC, Netherlands) Marie José Kersten (Amsterdam UMC, University of Amsterdam, Netherlands) Steven Pals (Amsterdam University Medical Centers, Location AMC, Netherlands) Hendrik Veelken (Leiden University Medical Center, Netherlands) Judith Bovee (Leiden University Medical Center, Netherlands) Arjen Cleven (Leiden University Medical Center, Netherlands) Joost Vermaat (Leiden University Medical Center, Netherlands)

Abstract:
Primary bone diffuse large B-cell lymphoma (PB-DLBCL) is a rare extranodal lymphoma subtype. This retrospective study elucidates the currently unknown genetic background of a large clinically well-annotated cohort of DLBCL with osseous localizations (O-DLBCL), including PB-DLBCL. 103 O-DLBCL patients were included and compared with 63 (extra)nodal non-osseous (NO)-DLBCLs with germinal center B-cell phenotype (NO-DLBCL-GCB). Cell-of-origin (COO) was determined by immunohistochemistry and gene-expression-profiling (GEP) using (extended)-NanoString/Lymph2Cx. Mutational profiles were identified with targeted next-generation deep-sequencing, including 52 B-cell lymphoma-relevant genes. O-DLBCLs, including 34 PB-DLBCL, were predominantly classified as GCB-phenotype based on immunohistochemistry (74%) and NanoString analysis (88%). Unsupervised hierarchical clustering of an extended-NanoString/Lymph2Cx demonstrated significantly different GEP-clusters for PB-DLBCL as opposed to NO-DLBCL-GCB ($P<0.001$). Expression levels of 23 genes of two different targeted GEP-panels, indicated a centrocyte-like phenotype for PB-DLBCL, whereas NO-DLBCL-GCB showed a centroblast-like constitution. PB-DLBCL had significantly more frequent mutations in four GCB-associated genes, i.e. B2M, EZH2, IRF8, and TNFRSF14, compared to NO-DLBCL-GCB ($P=0.031$, $P=0.010$, $P=0.047$, and $P=0.003$). PB-DLBCL with its corresponding specific mutational profile were significantly associated with a superior overall survival compared to equivalent Ann Arbor limited-stage I/II NO-DLBCL-GCB ($P=0.011$). This study is the first to demonstrate that PB-DLBCL is characterized by a GCB-phenotype, with a centrocyte-like GEP-pattern and a GCB-associated mutational profile (both involved in immune surveillance) and a favorable prognosis. These novel biology-associated features provide evidence that PB-DLBCL represents a distinct extranodal DLBCL entity and its specific mutational landscape holds potential for targeted therapies (e.g. EZH2-inhibitors).

Conflict of interest: COI declared - see note

COI notes: M.J.K. has received honoraria/research funding from Kite Pharma, Millennium/Takeda, Mundipharma, Gilead Sciences, Bristol-Myers Squibb, Roche, Celgene, Novartis Pharmaceuticals Corporation, and Amgen. P.J.L has received honoraria/research funding from Takeda, Servier, Genmab, Roche, Genentech, Celgene, Incyte, Regeneron The other authors do not have any conflict of interest or disclosure to declare: R.A.G., R.E., S.B., T.W., R.R., D.R., P.M.J., I.B.B., F.A.G., K.K., L.B., V.T., H.L., A.N., E.F.P., I.F.S., L.H., W.C.H., L.H.B., P.C.H., A.B., A.D., M.N., S.T.P., H.V., J.V.B., A.H.C., and J.S.V..

Preprint server: No;

Author contributions and disclosures: Histopathological samples were provided by P.M.J., V.T., A.N., I.F., W.C.H., P.C.H., S.T.P., A.D., J.V.B, and A.H.G.C.. Pathology review was performed by P.M.J., V.T.,

A.N., I.F., W.C.H., P.C.H., S.T.P., A.D., J.V.B, and A.H.G.C.. R.A.G., R.E., T.W., D.R., F.A.G., K.K. and I.B.B. gathered data derived from targeted NGS and FISH. Gene-expression profiling with the NanoString and Lymph2Cx data-analysis was provided by A.B. and A.D. R.R. performed radiological review. Clinical data regarding patients with (non-)osseous DLBCL from other hospitals were kindly provided by L.B., H.L., L.H., F.A.G. L.H.B., E.F.M.P., L.H., M.N., P.J.L., M.J.K, and H.V.. Statistical analyses was performed by R.A.G., S.B., A.H.G.C. and J.S.P.V.. R.A.G., A.H.G.C, and J.S.P.V. wrote the manuscript. All authors approved the final manuscript.

Non-author contributions and disclosures: No;

Agreement to Share Publication-Related Data and Data Sharing Statement: All targeted NGS data are uploaed in https://www.ncbi.nlm.nih.gov/bioproject/browse/ with project number PRJNA681466

Clinical trial registration information (if any):

Frequent mutated *B2M, EZH2*, *IRF8*, and *TNFRSF14* in primary bone diffuse large B-cell lymphoma reflect a GCB phenotype

Ruben A.L. de Groen[1], Ronald van Eijk[2], Stefan Böhringer[3], Tom van Wezel[2], Richard Raghoo[4], Dina Ruano[2], Patty M. Jansen[2], Inge Briaire-de Bruijn[2], Fleur A. de Groot[1], Karin Kleiverda[2], Liane te Boome[5], Valeska Terpstra[6], Henriette Levenga[7], Alina Nicolae[8], Eduardus F.M. Posthuma[9], Isabelle Focke-Snieders[10], Lizan Hardi[11], Wietske C.E. den Hartog[12], Lara H. Bohmer[13], Pancras C.W. Hogendoorn[2], Anke van den Berg[14], Arjan Diepstra[14], Marcel Nijland[15], Pieternella J. Lugtenburg[16], Marie José Kersten[17,18,19], Steven T. Pals[17,19,20], Hendrik Veelken[1], Judith V.M.G. Bovée[2], Arjen H.G. Cleven[2], and Joost S.P. Vermaat[1,*]

[1] Department of Hematology, Leiden University Medical Center, Leiden, The Netherlands
[2] Department of Pathology, Leiden University Medical Center, Leiden, The Netherlands
[3] Department of Biomedical Data Sciences, Leiden University Medical Center, Leiden, The Netherlands
[4] Department of Radiology, Leiden University Medical Center, Leiden, The Netherlands
[5] Department of Internal Medicine, Haaglanden Medical Center, The Hague, The Netherlands
[6] Department of Pathology, Haaglanden Medical Center, The Hague, The Netherlands
[7] Department of Internal Medicine, Groene Hart Hospital, Gouda, The Netherlands
[8] Department of Pathology, Groene Hart Hospital, Gouda, The Netherlands
[9] Department of Internal Medicine, Reinier de Graaf Hospital, Delft, The Netherlands
[10] Department of Pathology, Reinier de Graaf Hospital, Delft, The Netherlands
[11] Department of Hematology, Alrijne Hospital, Leiderdorp, The Netherlands
[12] Department of Pathology, Alrijne Hospital, Leiderdorp, The Netherlands
[13] Department of Hematology, Haga hospital, The Hague, The Netherlands
[14] Department of Pathology and Medical Biology, University of Groningen, University Medical Center Groningen, Groningen, The Netherlands
[15] Department of Hematology, University of Groningen, University Medical Center Groningen, Groningen, The Netherlands
[16] Department of Hematology, Erasmus MC Cancer Institute, University Medical Center, Rotterdam, The Netherlands
[17] Lymphoma and Myeloma Center Amsterdam-LYMMCARE, Amsterdam, The Netherlands
[18] Department of Hematology, Amsterdam University Medical Centers, University of Amsterdam, The Netherlands
[19] Cancer Center Amsterdam
[20] Department of Pathology, Amsterdam University Medical Centers, University of Amsterdam, The Netherlands

*** Correspondence**
Joost S.P. Vermaat MD PhD Msc, Department of Hematology, Leiden University Medical Center, PO Box 9600, 2300 RC Leiden, The Netherlands. *E-mail:* j.s.p.vermaat@lumc.nl

Running title
Molecular characteristics of primary bone DLBCL

Key words
Bone, diffuse large B-cell lymphoma, molecular profiles, gene expression patterns, prognosis

Funding
This study is funded by the Stichting Fonds Oncologie Holland.

Total word count
4395

Key points

Main point #1: PB-DLBCL is characterized by GCB-phenotype, with centrocyte-like GEP-pattern, GCB-associated mutational profile and favorable prognosis.

Main point #2: These features indicates PB-DLBCL as a distinct extranodal DLBCL entity and its specific mutations holds potential for targeted therapies.

Abstract

Primary bone diffuse large B-cell lymphoma (PB-DLBCL) is a rare extranodal lymphoma subtype. This retrospective study elucidates the currently unknown genetic background of a large clinically well-annotated cohort of DLBCL with osseous localizations (O-DLBCL), including PB-DLBCL. 103 O-DLBCL patients were included and compared with 63 (extra)nodal non-osseous (NO)-DLBCLs with germinal center B-cell phenotype (NO-DLBCL-GCB). Cell-of-origin (COO) was determined by immunohistochemistry and gene-expression-profiling (GEP) using (extended)-NanoString/Lymph2Cx. Mutational profiles were identified with targeted next-generation deep-sequencing, including 52 B-cell lymphoma-relevant genes. O-DLBCLs, including 34 PB-DLBCL, were predominantly classified as GCB-phenotype based on immunohistochemistry (74%) and NanoString analysis (88%). Unsupervised hierarchical clustering of an extended-NanoString/Lymph2Cx demonstrated significantly different GEP-clusters for PB-DLBCL as opposed to NO-DLBCL-GCB (P<0.001). Expression levels of 23 genes of two different targeted GEP-panels, indicated a centrocyte–like phenotype for PB-DLBCL, whereas NO-DLBCL-GCB showed a centroblast-like constitution. PB-DLBCL had significantly more frequent mutations in four GCB-associated genes, i.e. *B2M*, *EZH2*, *IRF8*, and *TNFRSF14,* compared to NO-DLBCL-GCB (P=0.031, P=0.010, P=0.047, and P=0.003). PB-DLBCL with its corresponding specific mutational profile were significantly associated with a superior overall survival compared to equivalent Ann Arbor limited-stage I/II NO-DLBCL-GCB (P=0.011). This study is the first to demonstrate that PB-DLBCL is characterized by a GCB-phenotype, with a centrocyte-like GEP-pattern and a GCB-associated mutational profile (both involved in immune surveillance) and a favorable prognosis. These novel biology-associated features provide evidence that PB-DLBCL represents a distinct extranodal DLBCL entity and its specific mutational landscape holds potential for targeted therapies (*e.g.* EZH2-inhibitors).

Introduction

The World Health Organization (WHO) Classification of Soft Tissue and Bone recognizes primary bone lymphoma as a specific lymphoma entity, which is primarily represented by diffuse large B-cell lymphoma (DLBCL).[1] Primary bone DLBCL (PB-DLBCL) is a rare DLBCL-subtype, with a relative young median age at diagnosis (55 years)[2], and a favorable 5-year overall survival (mean OS: 82%).[2-9] Most patients present with symptoms of pain, bone fractures, localized swelling, or suspected periprosthetic joint infection.[10-13] Patients' physical performance can be affected as weight-bearing bones are commonly involved (*f.e.* femur, spine, and pelvis).[2,6,13]

Between studies, reported clinical characteristics and survival rates are diverse due to a lack of strict (anatomical) definitions and consequent proper classification of DLBCL with osseous involvement (O-DLBCL). As such, WHO-classification[1] and Messina *et al.*,[2] distinguish three different sub-entities: PB-DLBCL with a single bone lesion with or without regional involvement of lymph nodes, polyostotic-DLBCL with multifocal disease in a single bone or multiple affected bones only, and disseminated-DLBCL with ≥1 bone lesion(s) and ≥1 (extra)nodal localization(s). These O-DLBCL sub-entities illustrate patients' outcomes with a superior survival for PB-DLBCL and polyostotic-DLBCL compared to disseminated-DLBCL.[2]

Only a few small retrospective cohort studies have investigated the clinicopathologic characteristics of O-DLBCL. Examining cell-of-origin (COO) with immunohistochemistry (IHC) by Hans' algorithm[14], these studies identified a predominantly germinal center B-cell (GCB)-phenotype in ~60% of O-DLBCL (n=269 cases, pooled data from 10 studies).[5,13,15-22] Based on gene-expression-profiling (GEP), this was confirmed by Li *et al.*,[8] demonstrating a GCB-phenotype in 90% (n=155). Nonetheless, a comprehensive molecular characterization of O-DLBCL is currently missing.

To our knowledge, only two studies report genetic data explicitly collected from O-DLBCL. First, lack of *MYD88* L265P hotspot mutation was observed in O-DLBCLs (n=15).[20] Second, applying a limited targeted next-generation sequencing (t)(NGS) panel, activating mutations in *NOTCH1* and *KRAS* were identified in PB-DLBCL (n=1).[23] Due to limited number of studies, relatively small patient cohorts, and absence of comprehensive genetic analyses, there is a lack of knowledge regarding the genetic constitution of O-DLBCL. This is caused by the rarity of the disease, the difficulty in obtaining sufficient diagnostic tissue and the inability to attain proper molecular analysis of bone biopsies, as decalcification procedures leads to acquisition of DNA artifacts and complicates interpretation of sequencing results. Consequently, it is unclear whether the different O-DLBCL sub-entities reflect a separate molecular entity or rather a heterogeneous disease, as commonly assumed for DLBCL-NOS.[24-28]

Since the introduction of (targeted)NGS, evidence of genetic heterogeneity associated with histopathological and clinical features and anatomical localization of DLBCL-NOS has increased. Therefore, the revised (2016) WHO Classification of Tumours of Haematopoietic and Lymphoid Tissues[29] recognizes extranodal DLBCL with specific anatomy as separate entities, such as intravascular large B-cell lymphoma (IVLBCL), primary cutaneous DLBCL, leg type (PC-DLBCL-LT), and primary DLBCL of the central nervous system (PCNSL), commonly representing an activated B-cell (ABC)-phenotype.[30-36] Following this paradigm and due to their specific disease presentation and clinical behavior, we hypothesized that PB-DLBCL contains unique molecular characteristics. To address this, our study presents the first comprehensive GEP and targeted deep-sequencing analyses in a well-annotated and relatively large cohort of PB-DLBCL.

Methods

Patient characteristics

This retrospective study investigated 103 O-DLBCLs of which sufficient tumor DNA was available and were not included in our previous studies.[12,19,37-41] Patients were selected through a search of pathology surveys that reported osseous involvement and diagnosed between 2002 and 2020 at the Leiden University Medical Center (LUMC; n=48), Amsterdam University Medical Center, location AMC (n=11), Erasmus MC Cancer Institute (n=7), or affiliated non-academic hospitals (n=37). As an expert-center for tumors of soft tissue and bone, the LUMC contribution was enriched for O-DLBCLs. Figure-1A presents an overview of included cases.

Formalin-fixed and paraffin-embedded or fresh frozen tissue samples were obtained during diagnostic procedures (Supplemental Table-1). Based on different local standard procedures at time of initial diagnosis, staging was performed with either MRI-, CT- or PET(/CT)-scan (Supplemental Table-1) and reviewed by a radiologist expert (R.R.) to stratify cases according to WHO-definitions.[1,2] As comparator, we included 63 patients diagnosed between 2006-2020 with non-osseous DLBCL as considered by radiological assessments and a GCB-phenotype (NO-DLBCL-GCB) based on Hans' algorithm (Figure-1A). T-cell/histiocyte-rich DLBCL and Burkitt lymphoma were not included. All cases were classified according to Ann Arbor and the International Prognostic Index. The study was performed in accordance with the Dutch Code for Proper Secondary Use of Human Tissue, the local institutional board requirements and the revised Declaration of Helsinki (2008) and was approved with a waiver of consent by the LUMC's medical ethics committee (B16.048).

Immunohistochemistry and fluorescence *in situ* hybridization (FISH)

Following the latest WHO classification of lymphoid neoplasms[29], IHC and FISH analyses were performed (elaborated in Supplemental Methods). Briefly, IHC was determined with CD10, BCL6, and MUM1 antibodies for COO classification according to Hans' algorithm.[14] For O-DLBCLs, *MYC*, *BCL2*, and *BCL6* rearrangements were analyzed by FISH, using break-apart probes, as outlined before.[42] NO-DLBCL-GCBs were screened for *MYC* rearrangements and if present, *BCL2* and *BCL6* rearrangements were assessed. EBV status was determined by EBV encoded RNA *in situ* hybridization.

Gene-expression-profiling

GEP was performed with a NanoString system and an extended custom-made probe set, covering 20 genes of the Lymph2Cx-assay for COO classification and additionally 219 genes related to DLBCL (Supplemental Methods).[43-47] For COO classification, raw counts obtained by NanoString gene-expression analysis were uploaded at the Lymphoma/Leukaemia Molecular Profiling Project website for COO categorization (https://llmpp.nih.gov/LSO/LYMPHCX/lymphcx_predict.cgi).[48] Technical variation of NanoString nCounter results of each sample was removed using standardization based on the geometric mean of inherent positive controls in the assay. Next, a principal component analysis was performed as a quality control for identification of possible outliers and potential 'batch effects' introduced by NanoString cartridges (Supplemental Figure-1). Gene-expression data was normalized by using five Lymph2Cx housekeeping genes and the resulting data were analyzed with RStudio (R-3.6.3, including packages NanoStringNorm-1.2.1, glmnet-3.0-2, factoextra-1.0.6, ComplexHeatmap-2.2.0, dendextend-1.13.4, ggpubr-0.4.0, and scales-1.1.1). All 234 genes (excluding housekeeping genes) were used to identify GEP clusters within O-DLBCLs and NO-DLBCL-GCB. In total, BAGS(2CLINICS)-assays consist of 208 genes, overlapping 26 genes of our custom NanoString panel. Thirteen genes of BAGS(2CLINIC)-assays, most distinctive between centroblast and centrocyte B-cells, were included for further analysis. Additionally, another study recently reported a dark zone/light zone (DZ/LZ)-spatial signature consisting of 53 genes, overlapping eleven genes with our panel. Both limited-(BAGS(2CLINIC) and DZ/LZ-spatial signature)-assays -with only *MYC* overlapping- were separately employed to relatively assign centroblast-like or centrocyte-like phenotypes (Supplemental Figure-3).[49-51] The gene-expression profiling reported in this article have been deposited in the Gene Expression Omnibus database (accession number GSE176126) and can also be found in supplementary table 4.

Targeted next-generation deep-sequencing

After microdissection from deparaffinised 10µm sections (median tumor cells: 70%, range 20-90, Supplemental Table-1), total nucleic acid was isolated with the fully automated Tissue Preparation System (Siemens Healthcare Diagnostics), as described previously.[52] For fresh frozen biopsies, DNA was isolated from 25µm cryosections, with the QIAamp DNA Mini Kit (Qiagen). The in-house designed and validated LYMFv1 NGS panel is an Ion-Torrent based Ampliseq panel (ThermoFisher Scientific, Bleijswijk, Netherlands, elaborated in Supplemental Methods). The LYMFv1 panel contains 1362 amplicons, subdivided into two primer-pools and covers 52 B-cell lymphoma-relevant genes (Supplemental Table-2). Briefly, this panel was compiled from a comprehensive review of ~300 articles (until 2018) on frequencies and clinical relevance of aberrations in B-cell lymphomas. The LYMFv1 panel has an overlap of 73% (33 genes) with a proposed consensus tNGS panel for all mature lymphoid malignancies.[53] LYMFv1 libraries were either prepared with an Ion Chef System (ThermoFisher Scientific) or manually. The resulting libraries were sequenced on an Ion Torrent S5-system (ThermoFisher Scientific). Sequence reads were aligned to the human reference genome (GRCh37/hg19) using TMAP 5.07 software, with default parameters (https://github.com/iontorrent/TS).[54] Variants were called by Torrent Variant Caller. The average read count was 3015 (Range, 253-13988). Supplemental Table-1 lists average read counts per patient. Minimum thresholds for calling variants were ≥100 on-target reads and 10% variant allele frequency. Samples were excluded if deep-sequencing data provided an insufficient number of reads or the transition to transversion ratio was ≥5, indicating excess formalin fixation artefacts. All variants were annotated in the Geneticist Assistant NGS interpretive Workbench (SoftGenetics), into class 1-benign, class 2-likely benign, class 3-unknown significance, class 4-likely pathogenic or class 5-pathogenic.[55] Class 4 and 5 variants were designated as pathogenic mutations. Additionally, class 3 variants of unknown pathogenicity were interpreted as pathogenic mutations, in case of a high CADD-phred score (>25) and/or a pathogenic prediction from ≥2 of four selected prediction scores (Sift, Polyphen, LRT, and MutationTaster). Sequencing data obtained for O-DLBCL and NO-DLBCL-GCB subgroups were mutually compared. Additionally, a literature based-cohort of DLBCL-GCB was gathered from four large sequencing studies.[24-27] Corresponding Supplemental Tables (or a figure[24]) reporting COO subtypes and potential pathogenic variants were used to identify mutational frequencies in DLBCL-GCB cases, collecting in total 651 DLBCL-GCB cases.

Statistical analysis

Statistical analyses were performed using RStudio (R-3.6.3, packages: clustertend-1.4, cmprsk-2.2-10, ComplexHeatmap-2.2.0, dendextend-1.13.4, dynpred-0.1.2, factoextra-1.0.6, ggpubr-0.4.0, glmnet-3.0-2, NanoStringNorm-1.2.1, prodlim-2019.11.13, scales-1.1.1, and survival-3.1.11). Hierarchical clustering analysis on GEP-data was performed using Euclidean distance metric and Ward's minimum variance method for cluster formation. A penalized logistic regression model was applied to identify genes most differentially expressed between PB-DLBCL and NO-DLBCL-GCB.[56] This model was based on elastic-net regression for which a mixing parameter alpha of 0.10 was used. ANOVA was applied on gene-expression data of a selected set of 13 genes of the BAGS(2CLINIC)-assay and 11 genes of the DZ/LZ spatial signature. Fisher's exact or Students' t-test was applied for analyzing categorical or continuous variables among O-DLBCL subgroups and NO-DLBCL-GCB. Progression free survival (PFS) or OS were defined as date from initial diagnosis to date of progression and/or death by any cause. Patients were administratively censored after three years of follow-up or censored at last follow-up when there was no event. Kaplan-Meier method was used to determine median follow-up time and to construct survival curves and were compared with a Log-rank test. In case of a statistically significant p-value (<0.05), corresponding hazard ratio (HR) and 95% confidence intervals (CI) were calculated with a Cox proportional hazard model.

Results

Patient characteristics

O-DLBCLs were categorized into PB-DLBCL (n=41), polyostotic-DLBCL (n=14), and disseminated-DLBCL (n=48, Figure-1A/B).[17] Table-1 summarizes clinical characteristics of both O-DLBCL and NO-DLBCL-GCB sub-entities. Individual radiologic assessments and age-related bone localizations are described in Supplemental Results. Figure-1C/D displays exact anatomical (non)osseous localizations. Consistent with previous studies, the mean age at diagnosis for PB-DLBCL and polyostotic-DLBCL was (borderline) significantly lower (53 and 50 years) compared to disseminated-DLBCL (62 years; P=0.020 and P=0.068) and NO-DLBCL-GCB (64 years; P=0.003 and P=0.033).[2,6,7] Additionally, NO-DLBCL-GCBs were subdivided into only nodal (n=19), mixed (nodal and extranodal involvement, n=28), or solitary extranodal localization (n=16). Six extranodal NO-DLBCL-GCBs were diagnosed with PCNSL, considered as poor-risk advanced disease (Ann Arbor Stage-IV) and treated with high-dose methotrexate containing regimens. Most patients (n=150, 90%) were treated with curative intent by (R-)CHOP-based (immune-)polychemotherapy. Five patients died before treatment and for palliation, four patients received local radiotherapy only, or rituximab monotherapy. Median follow-up times for O-DLBCLs and NO-DLBCL-GCBs were respectively 40 and 20 months.

Pathological features

Figure-2 displays morphological examples and immunohistochemical characteristics of O-DLBCL. According to Hans classification, a GCB-phenotype was identified in 74% of O-DLBCL (70 out of 94 patients, Supplemental Table-3). Using NanoString/Lymph2Cx a GCB-phenotype was found in 88% of O-DLBCL (35/40 patients), an 'intermediate/unclassifiable'-phenotype in 10% (n=4), and an ABC-phenotype in 2% (n=1). Additionally, NanoString/Lymph2Cx showed a GCB-phenotype in 90% of NO-DLBCL-GCB (18/20 patients), one ABC-phenotype and one intermediate/unclassifiable-phenotype. Overall, the COO concordance between cases with both IHC and NanoString was 83% (50/60 cases).

Fluorescence *in situ* hybridization

The majority of O-DLBCL (83/103 cases) were screened for *MYC*/*BCL2*/*BCL6* rearrangements and EBV-status (Figure-3A). Due to technical failures, most likely caused by decalcification of bone material, analysis of all three rearrangements failed in 40% (33/82 cases). Therefore, only a descriptive analysis was performed. Approximately similar frequencies of rearrangements were identified in polyostotic-DLBCL, disseminated-DLBCL and NO-DLBCL-GCB, largely consistent with occurrences in DLBCL-GCBs in literature.[24,27,28,57] Compared to NO-DLBCL-GCB, *MYC*-/*BCL2*-rearrangements were observed at relatively low frequencies, while *BCL6*-rearrangements were more common (4%, 8%, and 31%, respectively) in PB-DLBCL, indicating that only *BCL6* rearrangements appear to be relevant for PB-DLBCL lymphomagenesis. A 'double/triple'-hit make-up characteristic for high-grade B-cell lymphoma (HGBCL) was observed in ten NO-DLBCL-GCB, and three disseminated-DLBCL, but not in PB-DLBCLs/polyostotic-DLBCLs. IHC MYC and BCL2 status for evaluating double expressers are described in Supplemental Results. No O-DLBCL (n=61) and only three NO-DLBCL-GCB were EBV-positive. Lack of EBV in these overall GCB-subtype DLBCLs is consistent with previous studies describing occurrence of EBV-positive DLBCLs mainly (in elderly) with an ABC-phenotype.[58]

Gene-expression-profiling

As the NanoString material was limited, GEP was performed on 63 randomly selected cases, of which ~20 ng/µl of RNA was available (Figure-1A; Supplemental Table-5). After excluding three failed measurements and two outliers (Supplemental Figure-1), clustering of GEP-data was performed on 58 cases, representing 23 PB-DLBCL, 5 polyostotic-DLBCL, 11 disseminated-DLBCL, and 19 NO-DLBCL-GCB. Using both FF and FFPE tissues for GEP analysis did not impact the identified difference between O-DLBCL and NO-DLBCL-GCB (Supplemental Figure-1E/4). This is consistent with previous studies showing a high correlation between GEP-data obtained from FF and FFPE tissues.[59-61] Unsupervised hierarchical clustering with GEP-data of an extended Lymph2Cx (234 genes) provided four different clusters (Cluster A-D; Supplemental Figure-2). The most significant difference was found between cluster A, allocating eight PB-DLBCL and one NO-DLBCL-GCB, and cluster B, with three PB-DLBCL and 12 NO-DLBCL-GCB (P<0.001). Cluster C was a mixture of O-DLBCL sub-entities and cluster D an agglomeration of O-DLBCL subtypes and NO-DLBCL-GCBs. Disseminated-DLBCL was observed across all four clusters, indicating its heterogeneity and wide variety in disease origins of individual cases.

To further discriminate GEP differences between PB-DLBCL and NO-DLBCL-GCB, a penalized logistic regression model was performed, assigning a significant set of 34 genes differentially expressed between PB-DLBCL and NO-DLBCL-GCB. Unsupervised clustering of these differential-expressed genes generated three clusters: (A) predominantly PB-DLBCLs, (B) an agglomeration of O-DLBCL subtypes and NO-DLBCL-GCB, and (C) mainly NO-DLBCL-GCBs (Figure-4). In contrast to NO-DLBCL-GCB, PB-DLBCL showed significantly increased expression (P<0.001) of immune response genes (*CTLA4* and *CXCL12*) and *HLA-A*, *HLA-C*, *HLA-E*, and *HLA-F*. Elevated expression levels of *ARID1A* and *SMARCA4* (both involved in chromosome organization) and *FOXO1* (a centroblast hallmark) were found in NO-DLBCL-GCB as compared to PB-DLBCL.[62-65]

Subsequently, to relatively distinguish between a centroblast-like or centrocyte-like phenotype of PB-DLBCL and NO-DLBCL-GCB cases, both limited BAGS(2CLINIC)-GEP- and DZ/LZ-spatial signature assays were assessed.[49-51] Expression levels of eight genes (62%) were significantly different between PB-DLBCL and NO-DLBCL-GCB (Supplemental Figure-3, P≤0.047). PB-DLBCL showed significantly higher expression of *BCL2A1* and *IL6R* (centrocyte-related), while NO-DLBCL-GCB showed significantly increased expression for *BCL6*, *MME*, *MYBL1*, *FOXO1*, *SMARCA4* and *TCL1A* (centroblast-related). Applying a limited-DZ/LZ spatial signature, nine genes showed significantly higher expression (*CD3E*, *CD4*, *CD8A*, *CTLA4*, *FAS*, *HLA-E*, *ITGB2*, *LAG3*, and *STAT1* for PB-DLBCL as compared to NO-DLBCL-GCB (Supplemental Figure-3C/D, P≤0.031), designating a centrocyte-like phenotype for PB-DLBCL. Despite these limited-BAGS(2CLINIC) and limited-DZ/LZ-spatial signature-analyses, both independently identified GEP differences indicated a possible centrocyte-like phenotype for PB-DLBCL and a conceivable centroblast-like constitution for NO-DLBCL-GCB, corroborating previous results by Li, *et al*.[8]

Targeted next-generation deep-sequencing

In total, 83 O-DLBCLs and 63 NO-DLBCL-GCB were successfully deep-sequenced. For 20 O-DLBCLs obtained NGS data were of insufficient quality due to DNA artifacts (Figure-1A). Pathogenic variants were identified in 49 genes (Figure-3A and Supplemental Table-5), with a median of four mutated genes per individual (range 0-12). Four known 'hotspot' mutations were elucidated, loss-of-function *B2M* p.M1* and *CD79B*, p.Y196*, and gain-of-function *EZH2* p.Y646* and *MYD88* p.L265P. In contrast to a prior study, our data revealed low frequencies of *MYD88* p.L265P mutation in O-DLBCLs.[20] Based on strict 'anatomical' WHO-definitions, the two most biologically different DLBCL sub-entities (*i.e.* PB-DLBCL and NO-GCB-DLBCL) were compared to explore potential differences. The mutational profile of PB-DLBCL included frequent mutations (≥25%) in *B2M, EZH2*^{Y646*}, *IRF8,* and *TNFRSF14* (loss-of-function) and differed significantly from NO-DLBCL-GCB, relatively lacking these mutations (P=0.031, P=0.010, P=0.047, and P=0.003, respectively; Figure-3C).

In contrast to PB-DLBCL, high occurrences (≥25%) of *KMT2D* and *TP53* aberrations were observed within NO-DLBCL-GCB (P=0.347 and P=0.325). Besides frequent mutations in *CREBBP*, *KMT2D*, *MYD88*, and *TNFRSF14*, *CARD11* was the most commonly mutated gene (36%) in polyostotic-DLBCL was (borderline) significantly higher compared to PB-DLBCL (P=0.085), disseminated-DLBCL (P=0.036), or NO-DLBCL-GCB (P=0.014), suggesting a biologically distinct subgroup. With frequent mutations in *TNFRSF14, KMT2D*, or *TP53* disseminated-DLBCL revealed similarities with molecular constitutions of both PB-DLBCL and NO-DLBCL-GCB. Additionally, focusing on 19 disseminated-DLBCL cases with bulky osseous disease (Figure-3), comparable mutational profiles as PB-DLBCL were identified with high frequencies of mutations in *B2M* (16%)*, EZH2* (26%))*, IRF8* (21%)*,* and *TNFRSF14* (42%)*,* suggesting that this lymphoma originated in bone.

Survival analyses

Consistent with the prognostic importance of IELSG-staging[2], PB-DLBCL and polyostotic-DLBCL demonstrated superior PFS/OS (P=0.018/P=0.039; Figure-5A/B), compared to disseminated-DLBCL, with 3-year OS-rates of 91% (95%-CI: 0.82-1.00), 100% (95%-CI: 1.00-1.00), and 76% (95%-CI: 0.63-0.90), respectively. No significant difference in PFS/OS was observed for extranodal, nodal, and mixed NO-DLBCL-GCB sub-entities (Figure-5C/D). PB-DLBCL demonstrated a significantly superior PFS/OS compared to equivalent Ann Arbor stage I/II NO-DLBCL-GCBs (P=0.003/P=0.011; Figure-5E/F). Between PB-DLBCL and NO-DLBCL-GCB, the mutational landscape differed significantly (P=0.002), as the majority of PB-DLBCLs (24/34) harbored ≥1 mutation in *B2M*, *EZH2*, *IRF8*, and *TNFRSF14*, compared to a minority of Stage I/II NO-DLBCL-GCB (7/25) with ≥1 these specific mutations. No difference was observed in the occurrence of mutations in *KMT2D* or *TP53* between PB-DLBCL (12/34) and NO-DLBCL-GCB (12/25, P=0.423). With respect to Ann Arbor Stage III/IV, disseminated-DLBCL and NO-DLBCL-GCB showed similar survival outcomes, although polyostotic-DLBCL demonstrated an improved PFS/OS (Figure-5G/H). Besides a prognostic impact for Ann Arbor, IPI and age, further univariate survival analyses demonstrated no remarkable survival differences for patients' characteristics, COO, rearrangements, or individual pathogenic variants, presumably due to low patient numbers and relatively low number of events (Supplemental Table-6).

Discussion

To our knowledge, this study is the first to provide a comprehensive and integrative evaluation of IHC, GEP, and targeted deep-sequencing in a clinically well-annotated and relatively large cohort of O-DLBCL patients. As previously described[8], IHC/NanoString confirmed a predominant GCB-phenotype in O-DLBCLs, across all sub-entities. Extended-Lymph2Cx-GEP analysis revealed significantly different clusters for PB-DLBCL specifically targeting immune surveillance genes, in contrast to NO-DLBCL-GCB with a focus on chromosome organization and reduction of p53 activity. Limited-BAGS(2CLINIC)- and DZ/LZ-spatial signature-analysis indicated a centrocyte-like phenotype for PB-DLBCL with a preferential origin in the early light zone of B-cell development, as opposed to a centroblast-like constitution (dark zone) for NO-DLBCL-GCB. Intriguingly, the predominant GCB-centrocyte-like phenotype in PB-DLBCL was supported by frequent mutations in GCB-associated genes (i.e. *B2M*, *EZH2, IRF8,* and *TNFRSF14)*. Additionally, although a favorable survival in general for DLBCL-GCB, PB-DLBCL with its corresponding specific mutational profile was significantly associated with a superior OS compared to equivalent Ann Arbor limited-stage I/II NO-DLBCL-GCB. Based on our data, we propose a model in which PB-DLBCL can be recognized as a distinct extranodal DLBCL, with a centrocyte-like GCB-phenotype, overexpression of immune response genes and a unique GCB-associated molecular constitution, thereby reflecting favorable prognosis (Figure-6).

Controversial O-DLBCL definitions complicate a meaningful comparison between individual studies, including small numbers of O-DLBCLs (n=4-63) and varying frequencies (25-86%) of IHC-based GCB-phenotypes.[5,13,15-21,66] Using Affymetrix GeneChip/BAGS2CLINIC-assay, Li *et al*.[8] demonstrated a GCB-phenotype in 90% of O-DLBCLs (n=155) and a centrocyte-like phenotype in a small subgroup (n=11).[8] Likewise, our extended-NanoString/Lymph2Cx-GEP showed significantly different GEP-clusters for PB-DLBCL and NO-DLBCL-GCB. Additionally, limited-BAGS(2CLINIC)- and DZ/LZ-spatial signature-analysis indicated a centrocyte-like phenotype for PB-DLBCL and a centroblast-like constitution for NO-DLBCL-GCB.[49-51] In PB-DLBCL, Li *et al*. demonstrated upregulation of major histocompatibility complex class I, extracellular matrix and adhesion, and tumor suppressor genes and downregulation of pro-oncogenes, compared to NO-DLBCL-GCB.[8] Furthermore, high expression of genes involved in the immune response (*CTLA4* and *CXCL12*) were identified in PB-DLBCL, and together with frequent mutations in *B2M* and *TNFRSF14*, they are important for immune surveillance. This suggests that evasion from immune surveillance is crucial for PB-DLBCL to survive in their osseous environment.[62,63,65,67-69] In contrast, NO-DLBCL-GCB showed higher expression of *ARID1A* and *SMARCA4* (chromosome organization through SWI/SNF complex), and both target *TP53* (DNA damage response) and *CDKN1A* (cell cycle inhibitor).[64,65,69] The frequent mutations in genes involved in epigenetics (*CREBBP* and *MEF2B*) and *TP53* mutations indicate that, unlike immune evasion in PB-DLBCL, survival of NO-DLBCL-GCB is critically dependent on deregulation of chromosome organization and reduction of p53 activity.[65,69] Increased expression of *BCL2A1* and *IL6R* indicated a centrocyte-like phenotype for PB-DLBCL. Upregulation of *BCL6*, *MME*, *MYBL1*, *SMARCA4* and *TCL1A* suggested a centroblast-like constitution for NO-DLBCL-GCB. Lastly, high expression of *FOXO1*, a centroblast hallmark and imperative for sustaining the germinal center (GC) dark zone[65,69], was specifically found in NO-DLBCL-GCB, thereby supporting a centroblast-like phenotype for NO-DLBCL-GCB, as opposed to low/average *FOXO1* expression in PB-DLBCL.

Comprehensive reviews by Pasqualucci and Mlynarczyk *et al.* independently provide an integral insight into the development of GC-derived B-cell lymphomas.[65,69] Following these established pathogenic principles, the frequently mutated GCB-associated genes, *B2M*, *EZH2*, *IRF8*, and *TNFRSF14* (≥1 present in 68% of PB-DLBCLs), are likely to play a crucial role in GC B-cell lymphomagenesis, as elucidated by our data. Frequent occurrence of mutations in chromatin modifiers (*EZH2* and *TNFRSF14*) were observed, and although similarities with follicular lymphoma, other genetic abnormalities such as *BCL2* translocations were less common in PB-DLBCL (2/25). Approximately a quarter of PB-DLBCL pertained a gain-of-function *EZH2* hotspot mutation (Y646*), that abrogates the terminal B-cell differentiation and cell cycle control.[70] EZH2 acts as an important GC regulator like BCL6, through silencing of genes by tri-methylation of lysine-27 of histone-3 within the PRC2 complex. As such, *EZH2* Y646* hyper-represses CKDN1A and IRF4, increasing proliferation and preventing differentiation towards an activated B-cell.[65] Consequently, compared to *EZH2*-wildtype, *EZH2*-mutated DLBCL appears to be susceptible to tazemetostat (EZH2-inhibitor).[69,71] Moreover, *B2M* loss-of-function, *EZH2* gain-of-function aberrations and downregulation of MHC class I/II, will lead to a successful evasion of immune surveillance mechanisms.[65,69,72,73] *TNFRSF14* loss-of-function mutations are associated with B- and T-Lymphocyte Attenuator downregulation, thereby initiating a B-cell autonomous activation and lymphoma-supportive microenvironment.[69,74,75] Finally, IRF8 is a member of the interferon family of transcription factors, regulating immune response through BCL6 activation. However, an IRF8-driven phenotype alone is insufficient for lymphomagenesis as a second genetic hit is required.[76,77] This is consistent with our findings indicating that 57% (12/21) of mutated *IRF8* cases were accompanied by ≥1 *B2M, EZH2* and/or *TNFRSF14* abnormalities.

Four NGS studies investigated the mutational landscape of large DLBCL cohorts and also reported on COO (Affymetrix, IHC, and/or NanoString), allowing direct comparison of mutation frequencies in COO-stratified subgroups with our results in O-DLBCL.[24-27] These studies included 96, 60, 331, and 164 DLBCL-GCB cases, respectively. This pooled literature-based DLBCL-GCB cohort (n=651) yields mutation frequencies for *B2M*, *EZH2*, *IRF8*, *KMT2D*, *TNFRSF14*, and *TP53* of respectively 15%, 16%, 14%, 32%, 21%, and 15% (Figure-3C). Except for *EZH2* and *TNFRSF14* (P=0.148 and P=0.136), the occurrence of mutations in *B2M*and *IRF8*, in our cohort of PB-DLBCL were significantly higher as compared to the literature-based DLBCL-GCB cohort (P=0.012, and P=0.020, respectively). As essential data regarding exact anatomical localizations (ignorant for osseous involvement) was lacking for these studies, and control for confounding factors was not possible, it could be assumed that a proportion of DLBCL-GCBs were PB-DLBCLs. Excluding these cases from this literature-based cohort might increase the significance level of this comparison. Although an independent validation study remains indispensable, this external literature-based reflection strengthens our findings by emphasizing that PB-DLBCL could be recognized as a distinct molecular entity characterized by frequent mutations in *B2M*, *EZH2*, *IRF8*, and *TNFRSF14*, as compared to NO-DLBCL-GCB.

Clustering analyses in mentioned NGS studies have independently designated different (and partially overlapping) molecular DLBCL subtypes related to COO, prognosis, and potential therapeutic targets. In our study, the limited tNGS panel used for sequencing and lack of chromosomal aberrations impaired proper molecular classification of O-DLBCL subtypes. As such, Supplemental Table-7 summarizes only a derivative of these clusters related to identified molecular profiles in O-DLBCL sub-entities. Considering frequent mutations in *B2M*, *EZH2*, *IRF8*, and *TNFRSF14*, PB-DLBCL could primarily be categorized in 'good-risk' clusters (*e.g.* C1, C3, EZB, BN2, and BCL2), which corroborates our results for PB-DLBCL associated with favorable survival. This contrasts with other WHO-recognized extranodal DLBCLs, such as PCNSL, PCDLBCL-LT, and IVLBCL, which are primarily characterized by ABC-phenotypes and inferior survival. Our findings in PB-DLBCL coincides with compelling evidence, illustrating superior OS for DLBCL-GCB compared to DLBCL-ABC.[2,30-36]

The characterized genetic background of PB-DLBCL does not answer the question whether a lymphoma originates in the bone, since it is assumed that a GC does not exist in bones, or that circulating lymphoma cells are attracted by locally secreted chemokines. The contrast in mutational profiles between PB-DLBCL and NO-DLBCL-GCB (and even more with opposite extranodal DLBCL-ABCs) requires additional investigation into the coherence of these genetic factors and the resulting specific interactions with its microenvironment. Remarkably, no specific (extranodal) DLBCL-GCB entity has yet been recognized in the WHO Classification of Tumours of Haematopoietic and Lymphoid Tissues and therefore this study can be used as a reference study for DLBCL-GCB. As stated before[78], our findings (re)affirm the supplementary merit of examining well-annotated homogeneous cohorts and invoke the need of additional in-dept evaluation of (extra)nodal DLBCLs.

This study was limited by a percentage of GEP (7%, n=3) and tNGS dropouts (19%, n=20) of the O-DLBCL cohort, illustrating difficulties in molecular analysis on decalcified bone tissue, with no indication that this dropout is selective for certain outcomes. By using IHC as primary COO classifier, several non-GCB IHC cases that harbor a late GCB phenotype are absent from our comparator NO-DLBCL-GCB cohort. Given the low percentage (9%) of dissimilar COO classification by IHC and NanoString in the original study[48], we anticipate that this may have possibly biased our results, but to a limited extent. Moreover, this investigation would have benefited from more extensive GEP measurements (*e.g.* complete BAGS2CLINIC-assay or DZ/LZ-spatial signature-assay) for refinement of COO clustering and comprehensive sequencing data (*e.g.* whole-exome-sequencing) to elucidate complete molecular profiles including copy number alterations or larger structural variations. Nevertheless, these techniques would also have been impeded by our perceived (partially) suboptimal DNA/RNA qualities. Furthermore, GEP analyses focused on the comparison of PB-DLBCL with NO-DLBCL-GCB and therefore the numbers of polyostotic-DLBCL and disseminated-DLBCL analyzed were underrepresented and requires additional research. A sensitivity analysis demonstrated that the inclusion of a relatively small number of HGBCLs did not significantly bias our results (Supplemental Results). Multivariate analyses showed that the heterogeneity in age, chemotherapy, or adjuvant radiotherapy did not confound our survival outcomes (Supplemental Results).

In conclusion, this study is the first to demonstrate that PB-DLBCL is characterized by a centrocyte-like GCB-phenotype, with a specific GEP-pattern and GCB-associated mutational profile (mainly *B2M*, *EZH2*, *IRF8*, and *TNFRSF14* mutations), both involved in immune surveillance, and associated with favorable survival. Consequently, these new biological findings provide evidence that PB-DLBCL can be recognized as a distinct extranodal DLBCL entity and holds potential for development of targeted therapies (*e.g.* EZH2-inhibitors or other epigenetic-modulating agents[69]) to ultimately improve patients' survival.

Data sharing statement

The gene-expression profiling reported in this article have been deposited in the Gene Expression Omnibus database (accession number GSE176126).

Acknowledgements

The authors would like to thank A. Stolk, D. van Egmond, E. de Winter, J. Neefjes, M. Suleiman Ibramoglu, and S. Somers, for their valuable technical assistance. We would like to acknowledge the support provided by Dr Staudt's Laboratory at NCI/NIH Bethesda, Maryland, USA, for online analysis of Lymph2Cx raw data for COO characterization.

Conflict of interest

M.J.K. has received honoraria/research funding from Kite Pharma, Millennium/Takeda, Mundipharma, Gilead Sciences, Bristol-Myers Squibb, Roche, Celgene, Novartis Pharmaceuticals Corporation, and Amgen. P.J.L has received honoraria/research funding from Takeda, Servier, Genmab, Roche, Genentech, Celgene, Incyte, Regeneron.
The other authors do not have any conflict of interest or disclosure to declare: R.A.G., R.E., S.B., T.W., R.R., D.R., P.M.J., I.B.B., F.A.G., K.K., L.B., V.T., H.L., A.N., E.F.P., I.F.S., L.H., W.C.H., L.H.B., P.C.H., A.B., A.D., M.N., S.T.P., H.V., J.V.B., A.H.C., and J.S.V.

Authorship contributions

Histopathological samples were provided by P.M.J., V.T., A.N., I.F., W.C.H., P.C.H., S.T.P., A.D., J.V.B, and A.H.G.C.. Pathology review was performed by P.M.J., V.T., A.N., I.F., W.C.H., P.C.H., S.T.P., A.D., J.V.B, and A.H.G.C.. R.A.G., R.E., T.W., D.R., F.A.G., K.K. and I.B.B. gathered data derived from targeted NGS and FISH. Gene-expression profiling with the NanoString and Lymph2Cx data-analysis was provided by A.B. and A.D. R.R. performed radiological review. Clinical data regarding patients with (non-)osseous DLBCL from other hospitals were kindly provided by L.B., H.L., L.H., F.A.G. L.H.B., E.F.M.P., L.H., M.N., P.J.L., M.J.K, and H.V.. Statistical analyses was performed by R.A.G., S.B., A.H.G.C. and J.S.P.V.. R.A.G., A.H.G.C, and J.S.P.V. wrote the manuscript. All authors approved the final manuscript.

Literature

1. Cleven AHG, Ferry JA (2020) 'Primary non-Hodgkin lymphoma of bone', WHO classification of tumours editorial board (ed.) *WHO Classification of Tumours,* 5th edition, Volume 3: Soft Tissue and Bone Tumours. Lyon: IARC, pp. 489.
2. Messina C, Christie D, Zucca E, Gospodarowicz M, Ferreri AJ. Primary and secondary bone lymphomas. *Cancer treatment reviews.* 2015;41(3):235-246.
3. Jawad MU, Schneiderbauer MM, Min ES, Cheung MC, Koniaris LG, Scully SP. Primary lymphoma of bone in adult patients. *Cancer.* 2010;116(4):871-879.
4. Pellegrini C, Gandolfi L, Quirini F, et al. Primary bone lymphoma: evaluation of chemoimmunotherapy as front-line treatment in 21 patients. *Clinical lymphoma, myeloma & leukemia.* 2011;11(4):321-325.
5. Wu H, Bui MM, Leston DG, et al. Clinical characteristics and prognostic factors of bone lymphomas: focus on the clinical significance of multifocal bone involvement by primary bone large B-cell lymphomas. *BMC cancer.* 2014;14:900.
6. Bruno Ventre M, Ferreri AJ, Gospodarowicz M, et al. Clinical features, management, and prognosis of an international series of 161 patients with limited-stage diffuse large B-cell lymphoma of the bone (the IELSG-14 study). *The oncologist.* 2014;19(3):291-298.
7. Tao R, Allen PK, Rodriguez A, et al. Benefit of consolidative radiation therapy for primary bone diffuse large B-cell lymphoma. *International journal of radiation oncology, biology, physics.* 2015;92(1):122-129.
8. Li X, Xu-Monette ZY, Yi S, et al. Primary Bone Lymphoma Exhibits a Favorable Prognosis and Distinct Gene Expression Signatures Resembling Diffuse Large B-Cell Lymphoma Derived From Centrocytes in the Germinal Center. *The American journal of surgical pathology.* 2017;41(10):1309-1321.
9. Cleven AHG, Hogendoorn PCW. Hematopoietic Tumors Primarily Presenting in Bone. *Surg Pathol Clin.* 2017;10(3):675-691.
10. Beal K, Allen L, Yahalom J. Primary bone lymphoma: treatment results and prognostic factors with long-term follow-up of 82 patients. *Cancer.* 2006;106(12):2652-2656.
11. Santos TMD, Zumarraga JP, Reaes FM, Macaneiro CJ, Baptista AM, Camargo OP. PRIMARY BONE LYMPHOMAS: RETROSPECTIVE ANALYSIS OF 42 CONSECUTIVE CASES. *Acta ortopedica brasileira.* 2018;26(2):103-107.
12. Heyning FH, Hogendoorn PC, Kramer MH, Holland CT, Dreef E, Jansen PM. Primary lymphoma of bone: extranodal lymphoma with favourable survival independent of germinal centre, post-germinal centre or indeterminate phenotype. *Journal of clinical pathology.* 2009;62(9):820-824.
13. de Leval L, Braaten KM, Ancukiewicz M, et al. Diffuse large B-cell lymphoma of bone: an analysis of differentiation-associated antigens with clinical correlation. *The American journal of surgical pathology.* 2003;27(9):1269-1277.
14. Hans CP, Weisenburger DD, Greiner TC, et al. Confirmation of the molecular classification of diffuse large B-cell lymphoma by immunohistochemistry using a tissue microarray. *Blood.* 2004;103(1):275-282.
15. Bhagavathi S, Micale MA, Les K, Wilson JD, Wiggins ML, Fu K. Primary bone diffuse large B-cell lymphoma: clinicopathologic study of 21 cases and review of literature. *The American journal of surgical pathology.* 2009;33(10):1463-1469.
16. Lima FP, Bousquet M, Gomez-Brouchet A, et al. Primary diffuse large B-cell lymphoma of bone displays preferential rearrangements of the c-MYC or BCL2 gene. *American journal of clinical pathology.* 2008;129(5):723-726.
17. Chisholm KM, Ohgami RS, Tan B, Hasserjian RP, Weinberg OK. Primary lymphoma of bone in the pediatric and young adult population. *Human pathology.* 2017;60:1-10.
18. Hayase E, Kurosawa M, Suzuki H, et al. Primary Bone Lymphoma: A Clinical Analysis of 17 Patients in a Single Institution. *Acta haematologica.* 2015;134(2):80-85.

19. Koens L, Heyning FH, Szepesi A, Matolcsy A, Hogendoorn PC, Jansen PM. Nuclear factor-kappaB activation in primary lymphoma of bone. *Virchows Archiv : an international journal of pathology.* 2013;462(3):349-354.
20. Xu Y, Li J, Ouyang J, et al. Prognostic relevance of protein expression, clinical factors, and MYD88 mutation in primary bone lymphoma. *Oncotarget.* 2017;8(39):65609-65619.
21. Zhang X, Zhu J, Song Y, Ping L, Zheng W. Clinical characterization and outcome of primary bone lymphoma: a retrospective study of 61 Chinese patients. *Scientific reports.* 2016;6:28834.
22. Adams H, Tzankov A, d'Hondt S, Jundt G, Dirnhofer S, Went P. Primary diffuse large B-cell lymphomas of the bone: prognostic relevance of protein expression and clinical factors. *Human pathology.* 2008;39(9):1323-1330.
23. Zaharie F, Pop LA, Petrushev B, et al. Next-generation sequencing-based characterization of the invasion by anatomical contiguity in a primary osseous diffuse large B-cell lymphoma. Correlation between the genetic profile of the malignancy and the clinical outcome of the patient. *Histology and histopathology.* 2019;34(6):663-670.
24. Chapuy B, Stewart C, Dunford AJ, et al. Molecular subtypes of diffuse large B cell lymphoma are associated with distinct pathogenic mechanisms and outcomes. *Nat Med.* 2018;24(5):679-690.
25. Karube K, Enjuanes A, Dlouhy I, et al. Integrating genomic alterations in diffuse large B-cell lymphoma identifies new relevant pathways and potential therapeutic targets. *Leukemia.* 2018;32(3):675-684.
26. Reddy A, Zhang J, Davis NS, et al. Genetic and Functional Drivers of Diffuse Large B Cell Lymphoma. *Cell.* 2017;171(2):481-494 e415.
27. Schmitz R, Wright GW, Huang DW, et al. Genetics and Pathogenesis of Diffuse Large B-Cell Lymphoma. *N Engl J Med.* 2018;378(15):1396-1407.
28. Lacy SE, Barrans SL, Beer PA, et al. Targeted sequencing in DLBCL, molecular subtypes, and outcomes: a Haematological Malignancy Research Network report. *Blood.* 2020;135(20):1759-1771.
29. Swerdlow SH, Campo E, Harris NL, Jaffe ES, Pileri SA, Stein H, Thiele J: WHO Classification of Tumour of Haematopoietic and Lymphoid Tissues, Revised 4th edition. 2017. IARC Press, Lyon..
30. Bödör C, Alpár D, Marosvári D, et al. Molecular Subtypes and Genomic Profile of Primary Central Nervous System Lymphoma. *Journal of Neuropathology & Experimental Neurology.* 2019;79(2):176-183.
31. Schrader AMR, Jansen PM, Vermeer MH, Kleiverda JK, Vermaat JSP, Willemze R. High Incidence and Clinical Significance of MYC Rearrangements in Primary Cutaneous Diffuse Large B-Cell Lymphoma, Leg Type. *The American journal of surgical pathology.* 2018;42(11):1488-1494.
32. Schrader AMR, Jansen PM, Willemze R, et al. High prevalence of MYD88 and CD79B mutations in intravascular large B-cell lymphoma. *Blood.* 2018;131(18):2086-2089.
33. Vajpayee N, Hussain J, Tolocica I, Hutchison RE, Gajra A. Expression of signal transducer and activator of transcription 3 (STAT3) in primary central nervous system diffuse large B-cell lymphoma: a retrospective analysis of 17 cases. *J Neurooncol.* 2010;100(2):249-253.
34. Camilleri-Broët S, Crinière E, Broët P, et al. A uniform activated B-cell-like immunophenotype might explain the poor prognosis of primary central nervous system lymphomas: analysis of 83 cases. *Blood.* 2006;107(1):190-196.
35. Grommes C, Pastore A, Palaskas N, et al. Ibrutinib Unmasks Critical Role of Bruton Tyrosine Kinase in Primary CNS Lymphoma. *Cancer Discov.* 2017;7(9):1018-1029.
36. Preusser M, Woehrer A, Koperek O, et al. Primary central nervous system lymphoma: a clinicopathological study of 75 cases. *Pathology.* 2010;42(6):547-552.

37. Hemingway F, Kashima TG, Mahendra G, et al. Smooth muscle actin expression in primary bone tumours. *Virchows Archiv : an international journal of pathology.* 2012;460(5):525-534.
38. Rajnai H, Heyning FH, Koens L, et al. The density of CD8+ T-cell infiltration and expression of BCL2 predicts outcome of primary diffuse large B-cell lymphoma of bone. *Virchows Archiv : an international journal of pathology.* 2014;464(2):229-239.
39. Heyning FH, Kroon HM, Hogendoorn PC, Taminiau AH, van der Woude HJ. MR imaging characteristics in primary lymphoma of bone with emphasis on non-aggressive appearance. *Skeletal radiology.* 2007;36(10):937-944.
40. Heyning FH, Jansen PM, Hogendoorn PC, Szuhai K. Array-based comparative genomic hybridisation analysis reveals recurrent chromosomal alterations in primary diffuse large B cell lymphoma of bone. *Journal of clinical pathology.* 2010;63(12):1095-1100.
41. Heyning FH, Hogendoorn PC, Kramer MH, et al. Primary non-Hodgkin's lymphoma of bone: a clinicopathological investigation of 60 cases. *Leukemia.* 1999;13(12):2094-2098.
42. Vermaat JS, Somers SF, de Wreede LC, et al. MYD88 mutations identify a molecular subgroup of diffuse large B-cell lymphoma with an unfavourable prognosis. *Haematologica.* 2019.
43. Scott DW, Mottok A, Ennishi D, et al. Prognostic Significance of Diffuse Large B-Cell Lymphoma Cell of Origin Determined by Digital Gene Expression in Formalin-Fixed Paraffin-Embedded Tissue Biopsies. *J Clin Oncol.* 2015;33(26):2848-2856.
44. Chan FC, Telenius A, Healy S, et al. An RCOR1 loss-associated gene expression signature identifies a prognostically significant DLBCL subgroup. *Blood.* 2015;125(6):959-966.
45. Monti S, Savage KJ, Kutok JL, et al. Molecular profiling of diffuse large B-cell lymphoma identifies robust subtypes including one characterized by host inflammatory response. *Blood.* 2005;105(5):1851-1861.
46. Carey CD, Gusenleitner D, Chapuy B, et al. Molecular classification of MYC-driven B-cell lymphomas by targeted gene expression profiling of fixed biopsy specimens. *J Mol Diagn.* 2015;17(1):19-30.
47. Keane C, Vari F, Hertzberg M, et al. Ratios of T-cell immune effectors and checkpoint molecules as prognostic biomarkers in diffuse large B-cell lymphoma: a population-based study. *Lancet Haematol.* 2015;2(10):e445-455.
48. Scott DW, Wright GW, Williams PM, et al. Determining cell-of-origin subtypes of diffuse large B-cell lymphoma using gene expression in formalin-fixed paraffin-embedded tissue. *Blood.* 2014;123(8):1214-1217.
49. Michaelsen TY, Richter J, Brondum RF, et al. A B-cell-associated gene signature classification of diffuse large B-cell lymphoma by NanoString technology. *Blood Adv.* 2018;2(13):1542-1546.
50. Dybkaer K, Bogsted M, Falgreen S, et al. Diffuse large B-cell lymphoma classification system that associates normal B-cell subset phenotypes with prognosis. *J Clin Oncol.* 2015;33(12):1379-1388.
51. Tripodo C, Zanardi F, Iannelli F, et al. A Spatially Resolved Dark- versus Light-Zone Microenvironment Signature Subdivides Germinal Center-Related Aggressive B Cell Lymphomas. *iScience.* 2020;23(10):101562.
52. van Eijk R, Stevens L, Morreau H, van Wezel T. Assessment of a fully automated high-throughput DNA extraction method from formalin-fixed, paraffin-embedded tissue for KRAS, and BRAF somatic mutation analysis. *Exp Mol Pathol.* 2013;94(1):121-125.
53. Sujobert P, Le Bris Y, de Leval L, et al. The Need for a Consensus Next-generation Sequencing Panel for Mature Lymphoid Malignancies. *Hemasphere.* 2019;3(1):e169.
54. Cohen D, Hondelink LM, Solleveld-Westerink N, et al. Optimizing Mutation and Fusion Detection in NSCLC by Sequential DNA and RNA Sequencing. *J Thorac Oncol.* 2020;15(6):1000-1014.

55. Thompson BA, Spurdle AB, Plazzer JP, et al. Application of a 5-tiered scheme for standardized classification of 2,360 unique mismatch repair gene variants in the InSiGHT locus-specific database. *Nat Genet.* 2014;46(2):107-115.
56. Friedman J, Hastie T, Tibshirani R. Regularization Paths for Generalized Linear Models via Coordinate Descent. *J Stat Softw.* 2010;33(1):1-22.
57. Scherer F, Kurtz DM, Newman AM, et al. Distinct biological subtypes and patterns of genome evolution in lymphoma revealed by circulating tumor DNA. *Sci Transl Med.* 2016;8(364):364ra155.
58. Vockerodt M, Vrzalikova K, Ibrahim M, et al. Regulation of S1PR2 by the EBV oncogene LMP1 in aggressive ABC-subtype diffuse large B-cell lymphoma. *J Pathol.* 2019;248(2):142-154.
59. Ragulan C, Eason K, Fontana E, et al. Analytical Validation of Multiplex Biomarker Assay to Stratify Colorectal Cancer into Molecular Subtypes. *Scientific reports.* 2019;9(1):7665.
60. Sun J, Chen DT, Li J, et al. Development of Malignancy-Risk Gene Signature Assay for Predicting Breast Cancer Risk. *J Surg Res.* 2020;245:153-162.
61. Vukmirovic M, Herazo-Maya JD, Blackmon J, et al. Identification and validation of differentially expressed transcripts by RNA-sequencing of formalin-fixed, paraffin-embedded (FFPE) lung tissue from patients with Idiopathic Pulmonary Fibrosis. *BMC Pulm Med.* 2017;17(1):15.
62. Durr C, Pfeifer D, Claus R, et al. CXCL12 mediates immunosuppression in the lymphoma microenvironment after allogeneic transplantation of hematopoietic cells. *Cancer Res.* 2010;70(24):10170-10181.
63. Herrmann A, Lahtz C, Nagao T, et al. CTLA4 Promotes Tyk2-STAT3-Dependent B-cell Oncogenicity. *Cancer Res.* 2017;77(18):5118-5128.
64. Lunning MA, Green MR. Mutation of chromatin modifiers; an emerging hallmark of germinal center B-cell lymphomas. *Blood Cancer J.* 2015;5:e361.
65. Pasqualucci L. Molecular pathogenesis of germinal center-derived B cell lymphomas. *Immunol Rev.* 2019;288(1):240-261.
66. Shen H, Wei Z, Zhou D, et al. Primary extra-nodal diffuse large B-cell lymphoma: A prognostic analysis of 141 patients. *Oncology letters.* 2018;16(2):1602-1614.
67. Nijland M, Veenstra RN, Visser L, et al. HLA dependent immune escape mechanisms in B-cell lymphomas: Implications for immune checkpoint inhibitor therapy? *Oncoimmunology.* 2017;6(4):e1295202.
68. Boice M, Salloum D, Mourcin F, et al. Loss of the HVEM Tumor Suppressor in Lymphoma and Restoration by Modified CAR-T Cells. *Cell.* 2016;167(2):405-418 e413.
69. Mlynarczyk C, Fontan L, Melnick A. Germinal center-derived lymphomas: The darkest side of humoral immunity. *Immunol Rev.* 2019;288(1):214-239.
70. Morin RD, Johnson NA, Severson TM, et al. Somatic mutations altering EZH2 (Tyr641) in follicular and diffuse large B-cell lymphomas of germinal-center origin. *Nat Genet.* 2010;42(2):181-185.
71. Sarkozy C, Morschhauser F, Dubois S, et al. A LYSA Phase Ib Study of Tazemetostat (EPZ-6438) plus R-CHOP in Patients with Newly Diagnosed Diffuse Large B-Cell Lymphoma (DLBCL) with Poor Prognosis Features. *Clin Cancer Res.* 2020;26(13):3145-3153.
72. El Hussein S, Shaw KRM, Vega F. Evolving insights into the genomic complexity and immune landscape of diffuse large B-cell lymphoma: opportunities for novel biomarkers. *Modern pathology : an official journal of the United States and Canadian Academy of Pathology, Inc.* 2020.
73. Challa-Malladi M, Lieu YK, Califano O, et al. Combined genetic inactivation of beta2-Microglobulin and CD58 reveals frequent escape from immune recognition in diffuse large B cell lymphoma. *Cancer Cell.* 2011;20(6):728-740.
74. Steinberg MW, Cheung TC, Ware CF. The signaling networks of the herpesvirus entry mediator (TNFRSF14) in immune regulation. *Immunol Rev.* 2011;244(1):169-187.

75. Ennishi D, Hsi ED, Steidl C, Scott DW. Toward a New Molecular Taxonomy of Diffuse Large B-cell Lymphoma. *Cancer Discov.* 2020;10(9):1267-1281.
76. Qiu Z, Holder KN, Lin AP, et al. Generation and characterization of the Emicro-Irf8 mouse model. *Cancer genetics.* 2020;245:6-16.
77. Lee CH, Melchers M, Wang H, et al. Regulation of the germinal center gene program by interferon (IFN) regulatory factor 8/IFN consensus sequence-binding protein. *J Exp Med.* 2006;203(1):63-72.
78. Vermaat JS, Pals ST, Younes A, et al. Precision medicine in diffuse large B-cell lymphoma: hitting the target. *Haematologica.* 2015;100(8):989-993.

Figure-1 – Overview of included O-DLBCL and NO-DLBCL cohorts and sub-entities with specific anatomical localizations.

A) Flow-chart of included and analyzed O-DLBCL and NO-DLBCL sub-entities. 103 DLBCL cases with osseous involvement were subdivided into three O-DLBCL stages with primary bone (PB-)DLBCL (n=41), polyostotic-DLBCL (n=14), and disseminated-DLBCL (n=48). Of these, 20 cases failed tNGS quality controls (insufficient DNA or high number of deamination variants), whilst 83 cases attained appropriate sequencing results. In addition, 63 NO-DLBCL-GCB cases were included as comparator. Furthermore, 63 samples with adequate RNA were send for NanoString analysis, of which 3 failed analysis. In total 24 PB-DLBCL, 5 polyostotic-DLBCL, 11 disseminated-DLBCL, and 20 NO-DLBCL-GCB were successfully analyzed with the NanoString platform.

B) Radiological imaging of IELSG-staging system with three anatomically-defined stages: PB-DLBCL with a single bone lesion with or without regional involvement of lymph nodes, polyostotic lymphoma (polyostotic-DLBCL) with multifocal disease in a single bone or multiple affected bones, and disseminated lymphoma (disseminated-DLBCL) with ≥1 bone lesion(s) and ≥1 (extra)nodal localization(s).[2] NO-GCB-DLBCL was defined as nodal, mixed (nodal and extranodal involvement), or only extranodal localization(s), without any osseous involvement.

C) Frequencies of anatomical osseous localizations identified in all 103 O-DLBCL sub-entities. Other osseous localizations consisted of one calcaneus, cuneiform, metacarpal III, or talus.

D) Frequencies of anatomical non-osseous localizations of 63 NO-DLBCL-GCB.

Figure-2 - Morphological and immunohistochemical features of O-DLBCLs.

A) Infiltration of pleomorphic B-cells with entrapment of pre-existing bone (black arrowhead) in an example of PB-DLBCL.

B) Pleomorphic B cells in case of PB-DLBCL with large and irregular nuclei with a cleaved, multilobulated appearance and small nucleoli.

C) Pleomorphic B cells in case of disseminated-DLBCL with large nuclei and prominent large nucleoli with an immunoblastic/plasmablastic appearance.

D) Diffuse staining of CD20 in PB-DLBCL.

E) Diffuse staining of CD10 in an example of PB-DLBCL with a GCB phenotype, according to Hans' algorithm.

F) Strong diffuse staining of MUM1 in an example of disseminated-DLBCL with an ABC phenotype.

Figure-3 - Significant differences in genetic landscapes between PB-DLBCL and NO-DLBCL-GCB.

A) Oncoprintplot of the genetic aberrations and COO of O-DLBCL and (B) NO-DLBCL-GCB sub-entities. COO-phenotype is indicated by blue for ABC, orange for GCB, brown for intermediate (Only NanoString), and grey for cases with unknown COO-phenotype. Furthermore, a positive ISH (FISH or EBER) and a mutation in one of the genes are marked with green. Hotspot mutations are indicated with dark red (*B2M*^{M1*}, *CD79B*^{Y196*}, *EZH2*^{Y646*}, *MYD88*^{L265P}).

C) Comparison of identified genetic aberrations with high frequencies (≥20%) of PB-DLBCL, NO-DLBCL-GCB, and a pooled literature-based DLBCL-GCB cohort. PB-DLBCL showed a unique genetic profile with increased frequencies of *B2M*, *EZH2*, *IRF8*, and *TNFRSF14*, and was significantly different (P=0.031, P=0.010, P=0.047, and P=0.003) compared to NO-DLBCL-GCB harboring high occurrences (but not significant) of *KMT2D* and *TP53* aberrations (P=0.347 and P=0.325). Except for *EZH2* and *TNFRSF14* (P=0.148 and P=0.136), the occurrence of mutations in *B2M* and *IRF8*, in our cohort of PB-DLBCL were significantly higher compared to literature-based DLBCL-GCB cohort (P=0.012 and P=0.020, respectively). Careful interpretation is needed, as essential data regarding exact anatomical localizations (*e.g.* ignorant for osseous involvement) were lacking for these studies.

Figure-4 - Specific GEP-patterns for PB-DLBCL and NO-DLBCL-GCB.

A) A penalized logistic regression model assigned 34 differentially expressed genes between PB-DLBCL and NO-DLBCL-GCB. As shown in the heatmap, unsupervised hierarchical clustering of these differential-expressed genes generated three clusters: a cluster with predominant PB-DLBCLs, a cluster with an agglomeration of O-DLBCL sub-entities and NO-DLBCL-GCB, and a cluster with mainly NO-DLBCL-GCBs. In contrast to NO-DLBCL-GCB, PB-DLBCL showed significantly (P<0.001) increased expression of immune response genes (*CTLA4*, *CXCL12*, *HLA-A*, *HLA-C*, *HLA-E*, and *HLA-F*). Elevated expressions of *ARID1A* and *SMARCA4* (both involved in chromosome organization) and *FOXO1* (a centroblast hallmark) was found in NO-DLBCL-GCB, as opposed to low expressions in PB-DLBCL.

B) This bar chart demonstrates the distribution of the PB-DLBCL and NO-DLBCL-GCB sub-entities across elucidated clusters.

Figure-5 - Three-year PFS and OS analysis for O-DLBCL and NO-DLBCL-GCB sub-entities.

A/B) Consistent with the prognostic importance of IELSG-staging, PB-DLBCL and polyostotic-DLBCL demonstrated a significantly superior PFS and OS, compared to disseminated-DLBCL.

C/D) No significant difference in PFS or OS was shown for the subdivision of NO-DLBCL-GCB into extranodal, nodal, and mixed groups.

E/F) PB-DLBCL elucidated a significantly favorable PFS and OS, compared to equivalent Ann Arbor stage I/II NO-DLBCL-GCBs.

G/H) With respect to Ann Arbor Stage III/IV, there was no difference in PFS or OS, between disseminated-DLBCL and NO-DLBCL-GCB, although polyostotic-DLBCL demonstrated an improved survival.

Figure-6 – Mechanistical overview of germinal center B-cell development related to PB-DLBCL and NO-DLBCL-GCB and their identified specific GEP patterns and molecular profiles.

As described by Li *et al*. and corresponding with our GEP analysis demonstrating an increased expression of *BCL2A1* and *IL6R*, PB-DLBCL preferentially originated in the germinal center (GC) early light zone of B-cell development, indicating a centrocyte-like phenotype. The predominant centrocyte-like GCB-phenotype in PB-DLBCL was subsequently supported by frequently mutated GCB-associated genes, such as *B2M*, *EZH2, IRF8,* and *TNFRSF14*, culminating in superior survival. Additionally, PB-DLBCL showed significantly ($P<0.001$) increased expression of immune response genes (*CTLA4* and *CXCL12*), and together with frequent mutations in *B2M* and *TNFRSF14*, they are important for immune surveillance, suggesting that evasion from immune surveillance is crucial for PB-DLBCL to survive in their osseous environment. In contrast, upregulation of *BCL6*, *MME*, *MYBL1*, *SMARCA4* and *TCL1A* suggested a centroblast-like constitution for NO-DLBCL-GCB. Accordingly, high expression of *FOXO1*, a centroblast hallmark and imperative for sustaining the GC dark zone[62-65,69], was specifically identified in NO-DLBCL-GCB. Furthermore, elevated expression levels of *ARID1A* and *SMARCA4* (both involved in chromosome organization) were found in NO-DLBCL-GCB. Together with frequent mutations in genes involved in epigenetics (*CREBBP* and *MEF2B*) and *TP53* mutations, this indicates that, unlike immune evasion in PB-DLBCL, survival of NO-DLBCL-GCB is critically dependent on deregulation of chromosome organization and reduction of p53 activity. Summarized, our results emphasize that PB-DLBCL can be recognized as a distinct extranodal DLBCL, with a GCB-centrocyte-like phenotype, a specific GEP-pattern, and a unique GCB-associated molecular constitution, reflecting favorable prognosis. Purple color indicates genes related to a centroblast-like phenotype, whereas brown colored genes are related to a centrocyte-like phenotype.

Table-1 - Patient characteristics of DLBCL with osseous involvement (O-DLBCL) and non-osseous DLBCL-GCB (NO-DLBCL-GCB).

Characteristics	PB-DLBCL (N=41)		Polyostotic-DLBCL (N=14)		Disseminated-DLBCL (N=48)		Extranodal NO-DLBCL-GCB (N=16)		Nodal NO-DLBCL-GCB (N=19)		Mixed NO-DLBCL-GCB (N=28)	
Gender (Male)	24	59%	9	64%	32	67%	10	63%	13	68%	18	64%
Median age (min-max; Years)	54 (18-86)		56 (13-73)		63 (30-91)		65 (46-82)		67 (35-84)		63 (44-95)	
Ann Arbor												
I((X)E)	29	71%	0	0%	0	0%	4	25%	2	11%	0	0%
II((X)E)	12	29%	0	0%	3	6%	2	13%	9	47%	8	29%
III(E/S)	0	0%	0	0%	3	6%	0	0%	8	42%	2	7%
IV	0	0%	14	100%	42	88%	10	63%	0	0%	18	64%
IPI-score												
0-1	26	63%	3	21%	7	15%	6	38%	11	58%	8	29%
2-5	15	37%	11	79%	41	85%	10	63%	8	42%	20	71%
First line treatment												
R-CHOP +/- adjuvant radiotherapy*	35	85%	12	86%	42	88%	8	50%	16	84%	23	82%
Other chemotherapy +/- adjuvant radiotherapy†	4	10%	2	14%	4	8%	0	0%	1	5%	3	11%
High dose MTX‡ +/- adjuvant radiotherapy	0	0%	0	0%	0	0%	7	44%	0	0%	0	0%
Palliative treatment§	2	5%	0	0%	2	4%	1	6%	2	11%	2	7%
Response to first line treatment												
CR	37	90%	14	100%	36	75%	11	69%	14	74%	18	46%
non-CR	4	10%	0	0%	12	25%	5	31%	5	26%	10	36%
Therapy ongoing	0	0%	0	0%	0	0%	0	0%	0	0%	0	0%
Median follow-up (Months)	50		53		37		33		17		22	

* R-CHOP (rituximab, cyclophosphamide, doxorubicin, vincristine, and prednisone; N=136) and adjuvant radiotherapy (N=47)

† CHVmP/BV (cyclophosphamide, doxorubicin, teniposide and prednisone with bleomycin and vincristine at mid-interval; N=4), CHOP (N=1), COPADM (cyclophosphamide, vincristine, prednisone, doxorubicin, and methotrexate; N=1), DA-EPOCH-R (dose-adjusted etoposide, prednisolone, vincristine, cyclophosphamide, doxorubicin, rituximab; N=5), PECC (prednisone, etoposide, chlorambucil, and lomustine; N=1), RCEOP (rituximab, cyclophosphamide, etoposide, vincristine, and prednisone; N=1), RCVP (rituximab, cyclophosphamide, vincristine, prednisone; N=1), and adjuvant radiotherapy (N=9)

‡ MATRIX (high-dose methotrexate (MTX), cytarabine, thiotepa, rituximab)/BCNU (Carmustine)/autologous stem cell transplantation (N=1), MBVP (high-dose methotrexate, BCNU, teniposide, prednisone)/HD_araC (High dose ara-cytarabine) (N=1), or RMP (Rituximab, high-dose methotrexate, and procarbazine; N=5), and adjuvant radiotherapy (N=2)

§ Local radiotherapy (N=3), R-mono (N=1), or no treatment (N=5)

1

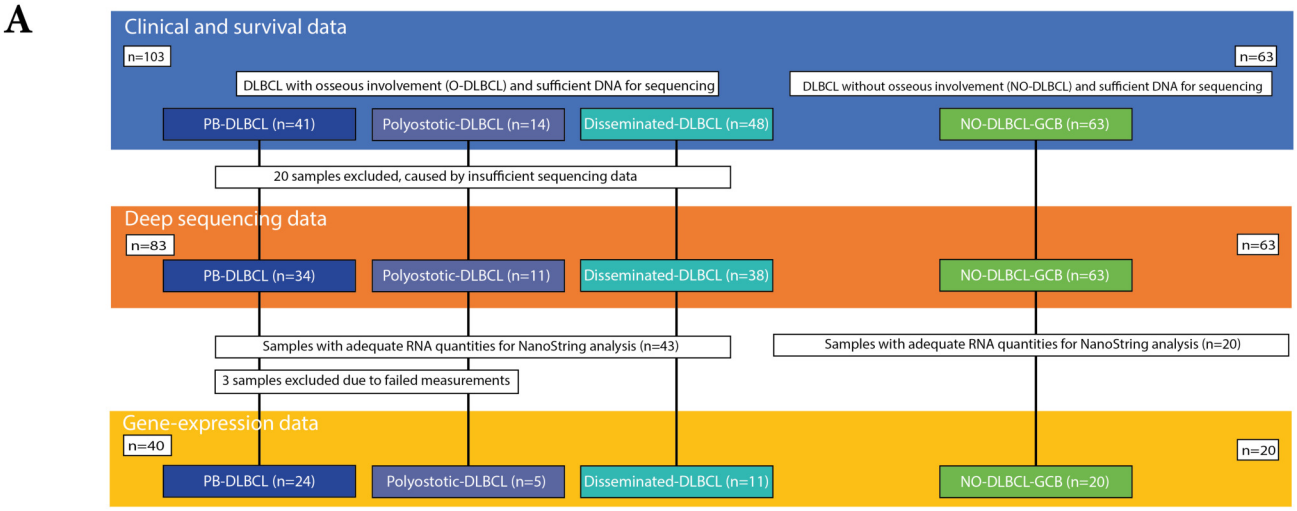

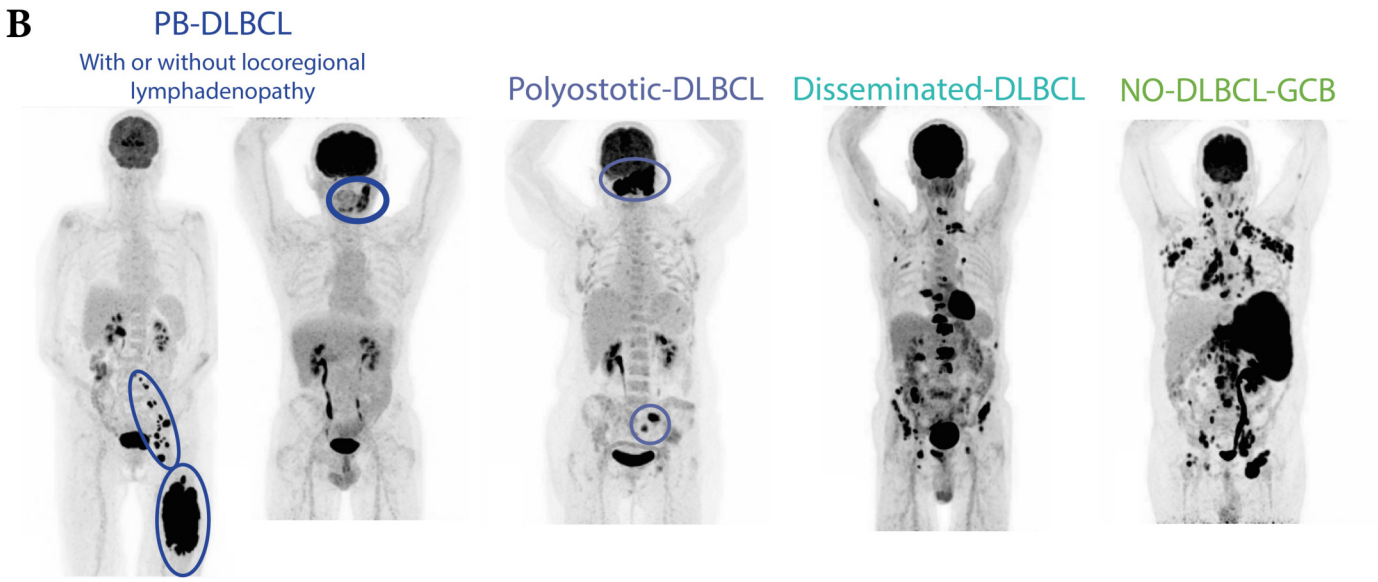

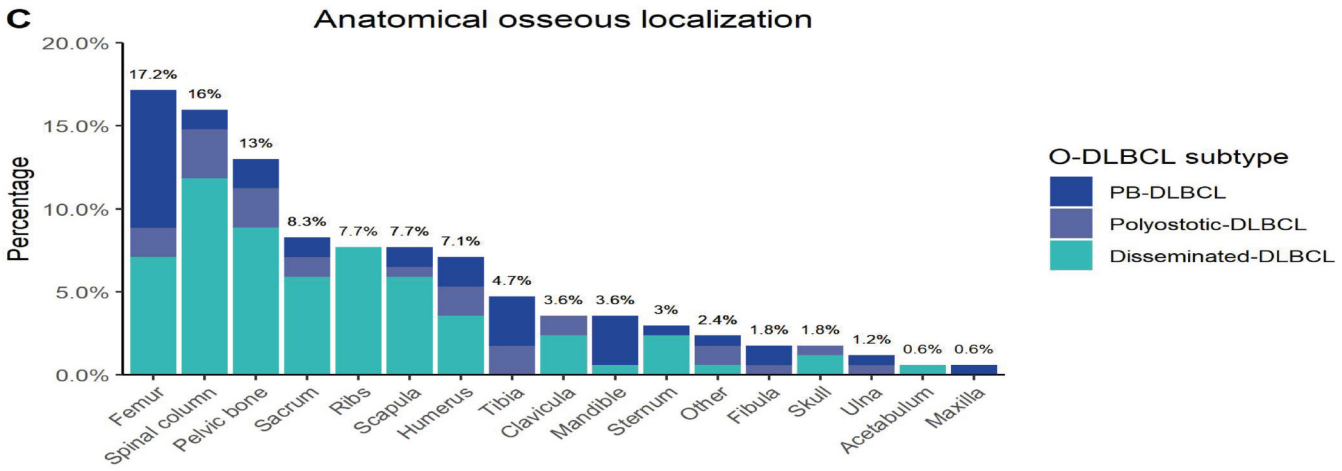

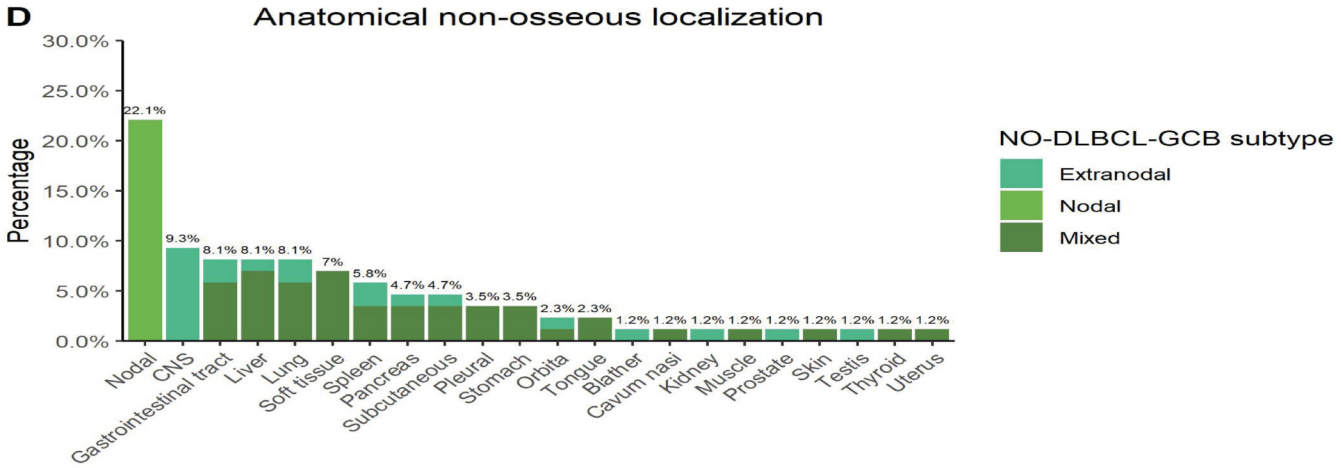

2

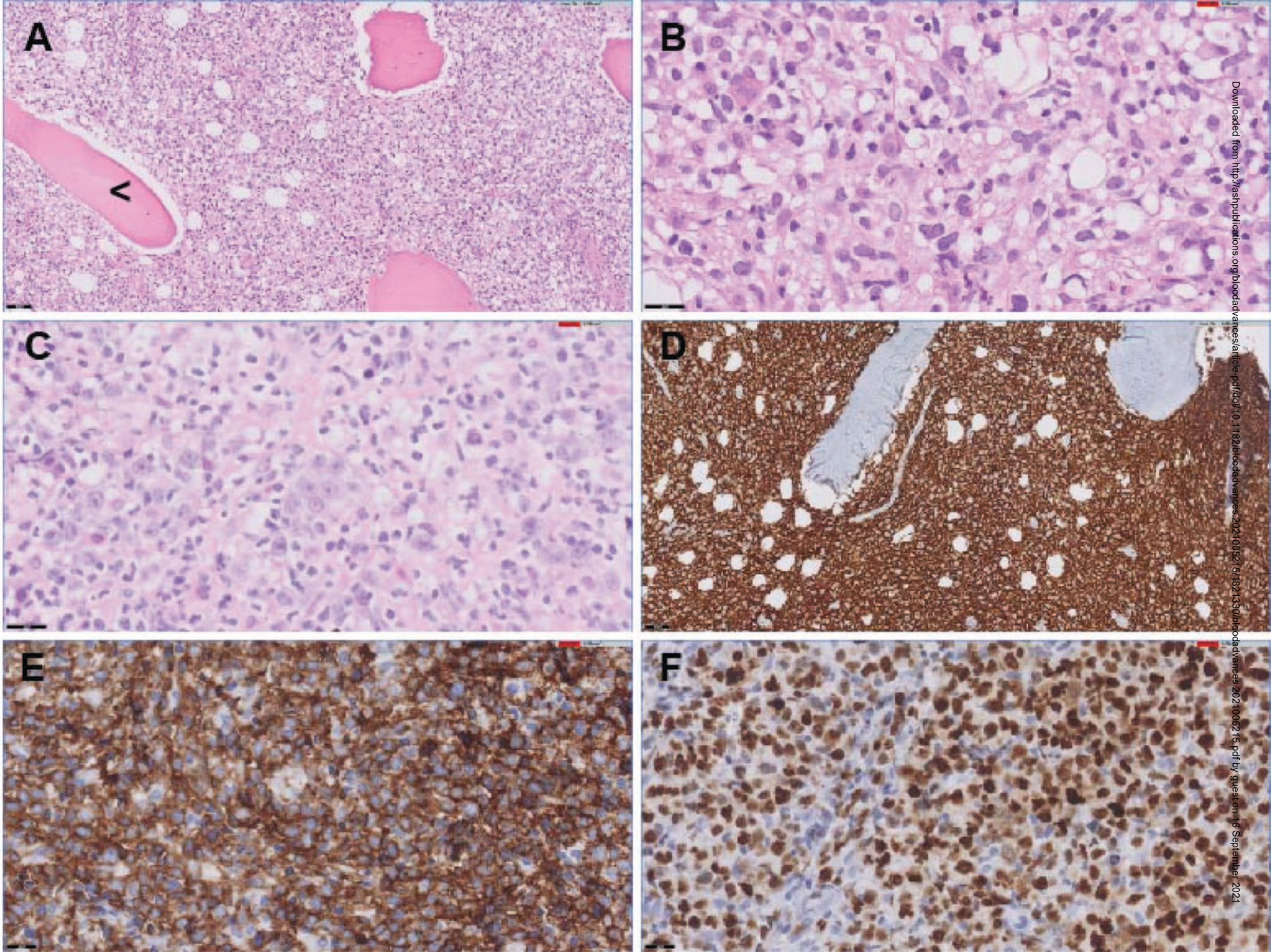

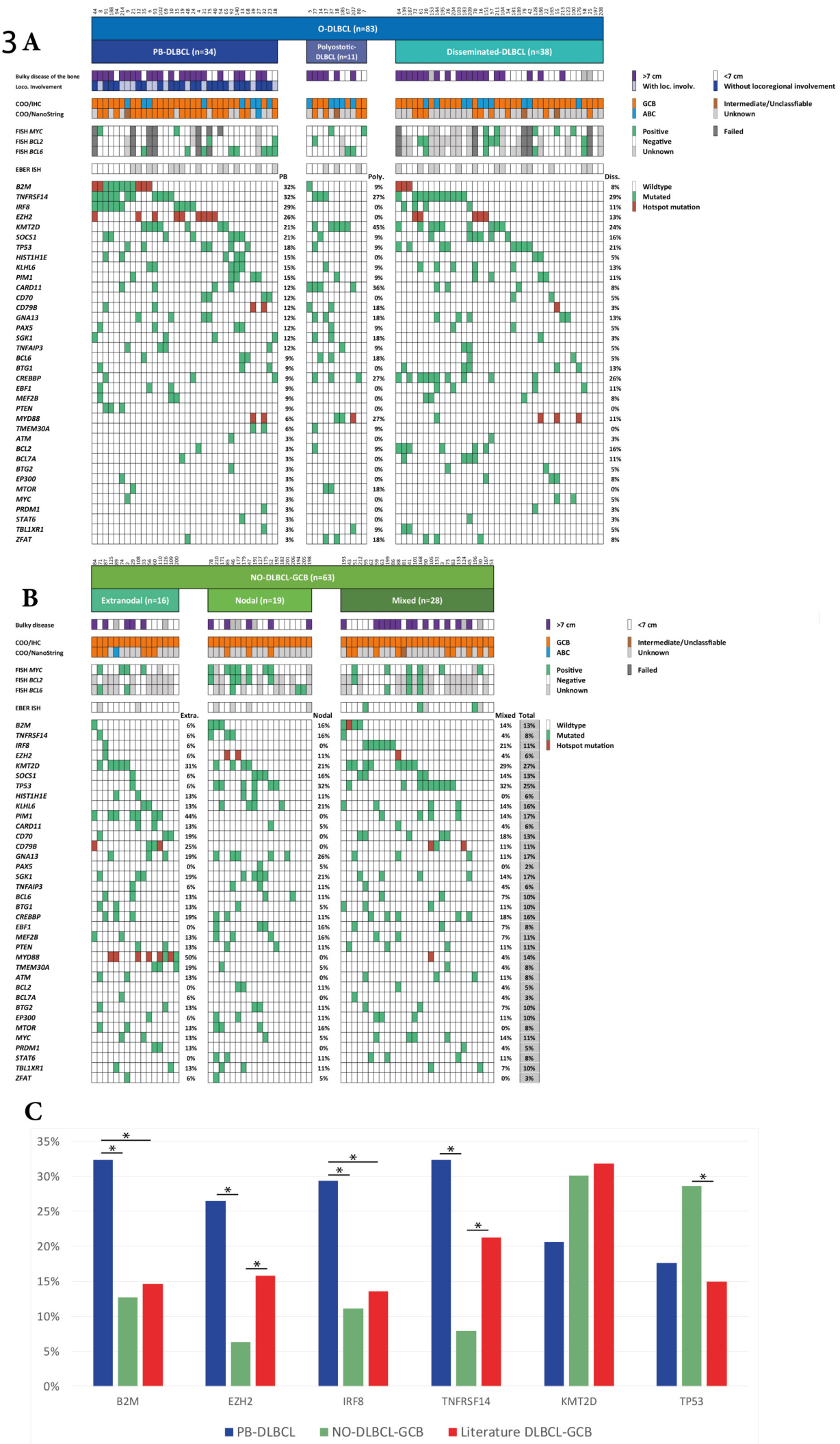

4

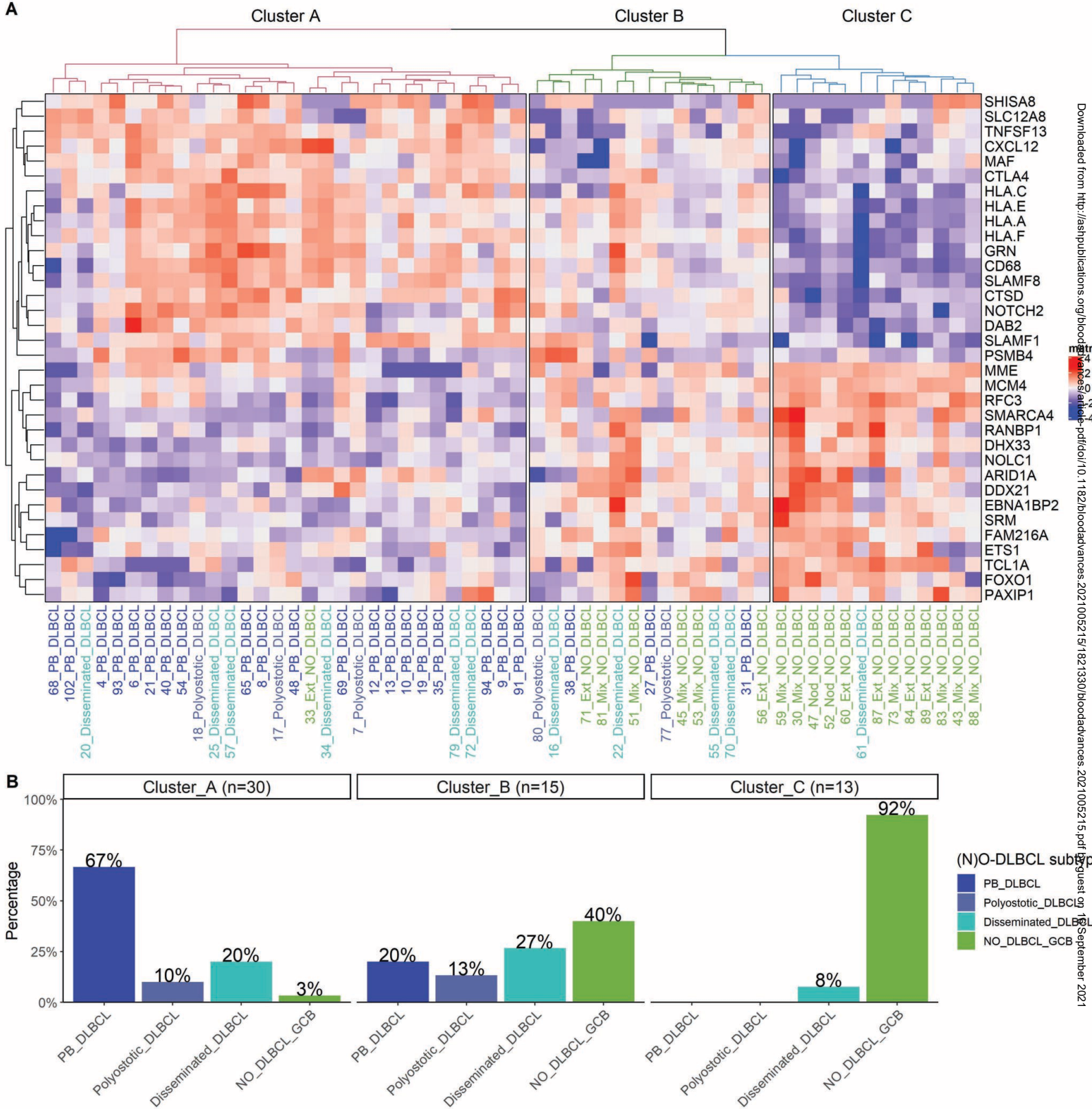

5 A

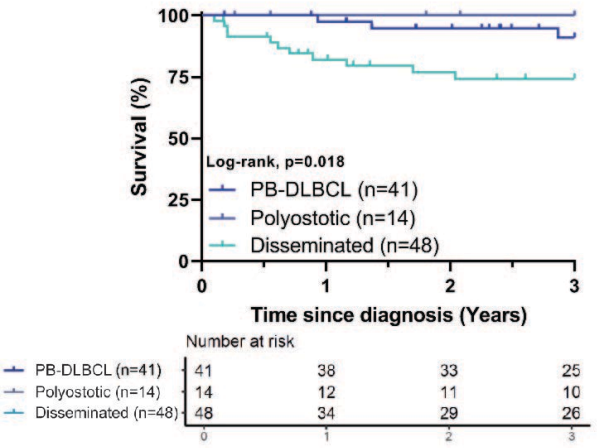

B

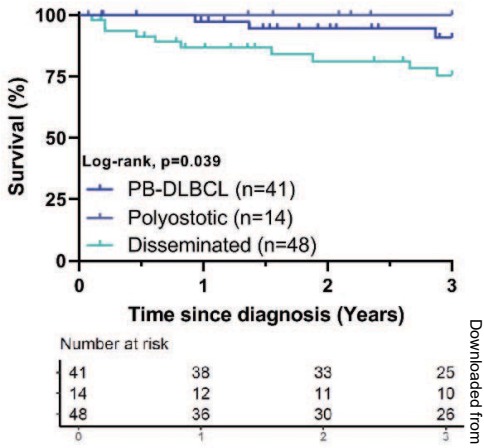

C

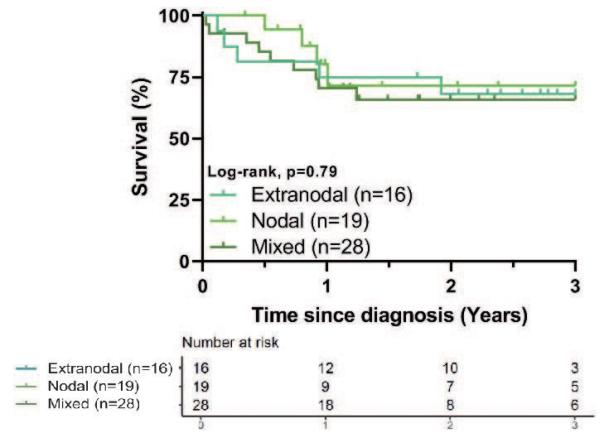

D

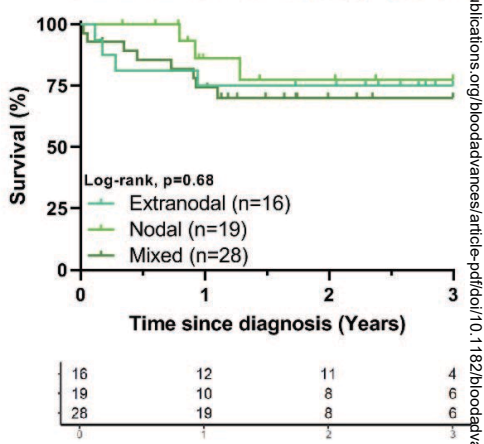

E

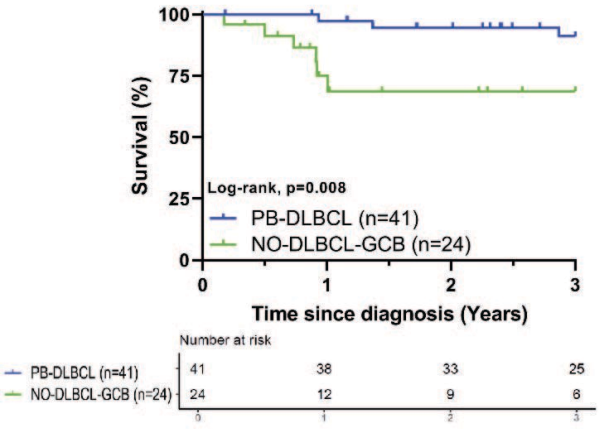

F

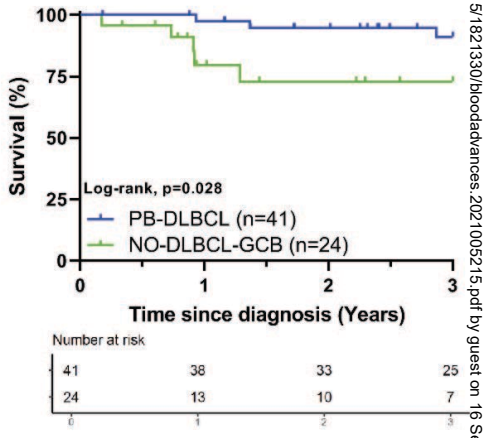

G

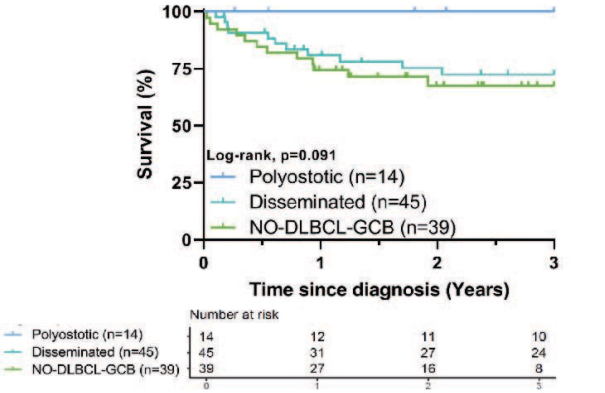

H

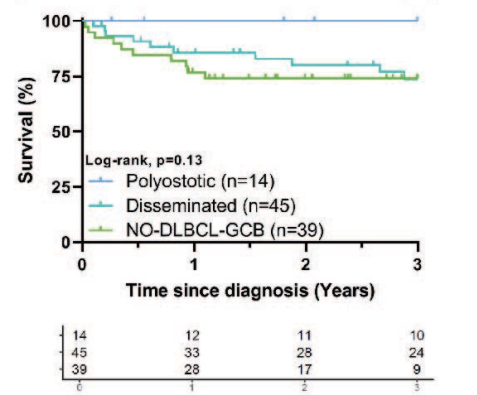

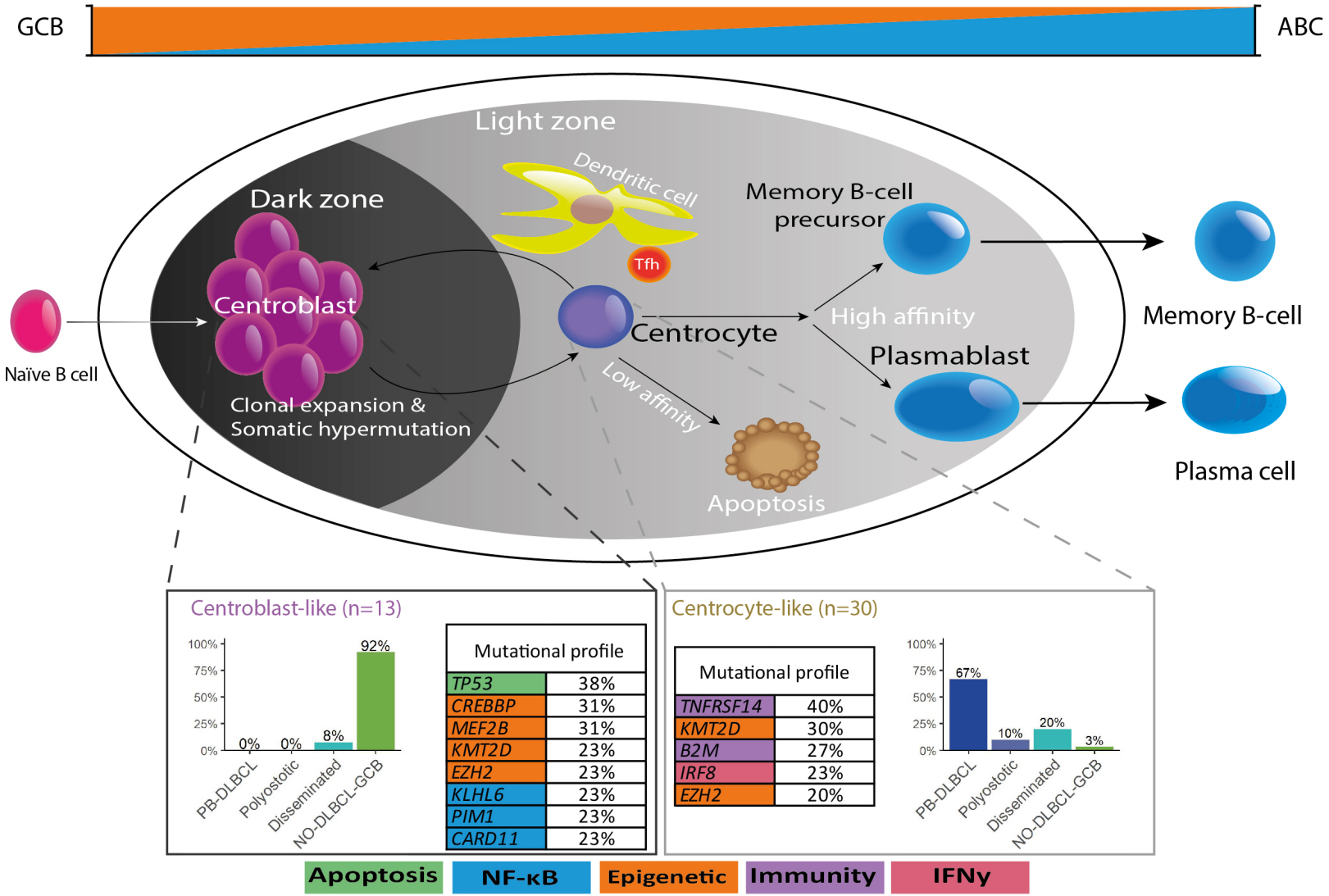

Gene-expression profile	
Function	Centroblast-like (n=13) vs centrocyte-like (n=30)
Apoptosis	↓: *BCL2A1*, *FAS*
Cell cycle	↑: *RANBP1*, *TCL1A*
Chromatin organization	↑: *ARID1A*
DNA-damage	↑: *PAXIP1*, *RFC3*
Gene expression	↑: *DDX21*, *DHX33*, *EBNA1BP2*, *ETS1*, *FOXO1*, *MYBL1*, *NOLC1* ↓: *MAF*
Immunity	↑: *MME*, *SMARCA4* ↓: *CD3E*, *CD4*, *CD8A*, *CD68*, *CTLA4*, *CTSD*, *CXCL12*, *HLA-A*, *HLA-C*, *HLA-E*, *HLA-F*, *IL6R*, *ITGB2*, *LAG3*, *SLAMF1*, *SLAMF8*
Proliferation, differentiation	↑: *BCL6*, *MCM4*, *MYC* ↓: *NOTCH2*, *STAT1*, *TNFSF13*
Protein metabolism	↑: *SRM* ↓: *PSMB4*, *GRN*
Other	↑: *FAM216A* ↓: *DAB2*, *SHISA8*, *SLC12A8*